156
23

NONLINEAR PID CONTROLLERS

by

Nicholas Durante Murray, Jr.

Thesis submitted to the Faculty of the

Virginia Polytechnic Institute and State University

in partial fulfillment of the requirements for the degree of

MASTER OF SCIENCE

in

Electrical Engineering

APPROVED:

W. T. Baumann, Chairman

W. F. VanLandingham

J. S. Bay

September, 1990

Blacksburg, Virginia

NONLINEAR PID CONTROLLERS

by

Nicholas D. Murray, Jr.

Committee Chairman: William T. Baumann

Electrical Engineering

(ABSTRACT)

An algorithm to design simple gain scheduled nonlinear PID controllers for nonlinear plants is investigated. Design information is obtained from measurements of the nonlinear plant about selected equilibrium points.

Simulations are performed on two different nonlinear CSTR models. The first simulation produced an unexpected result: that linear output feedback performed better than state feedback for the particular model. The second simulation showed that the nonlinear PID controller performed as well as a complex nonlinear controller.

A literature search for similar nonlinear controllers concluded that the nonlinear PID controller presented in this thesis did not provide a unified framework for previous work.

ACKNOWLEDGEMENTS

I would like to thank Dr. Baumann for his inspiration and guidance throughout this thesis. I would also like to thank Dr. VanLandingham for his advice (when I needed it the most), Chris Stewart for the state feedback controller information used in Chapter 3, and his girlfriend Wendy for feeding me (when I needed a good, home cooked meal).

Finally, I would like to thank my family for their support. I could not have come this far without it.

TABLE OF CONTENTS

TABLES

FIGURES

CHAPTER 1

Introduction

The study of nonlinear systems and the failure of linear controllers to adequately operate such systems over the wide range of interest has led to the development of nonlinear controllers that adapt themselves to changing plant dynamics. These controllers can vary widely in scope and complexity, depending on the approach to obtain a desirable control law. Practical application of such controllers, however, can be quite difficult and most plant operators don't trust new, sophisticated control schemes. This has generated interest in simplifying nonlinear controllers while maintaining reasonable system performance.

One approach to simplification has been modifying classical linear control structures so that they will operate over a wider range. A modification scheme that is routinely applied is a technique called 'gain scheduling', where the controller gains are varied with respect to a plant variable. The controller gains become nonlinear functions of a plant variable and result in a nonlinear form of a classical controller. The methods used in developing these nonlinear controllers, however, can still lead to complicated controller schemes and might require extensive plant testing before the controller can be implemented.

A nonlinear PID controller framework is presented in Rugh(1987). This framework involves gain scheduling the controller gains as a function of the plant input. After linearizing the nonlinear plant the controller gains are tuned using the Ziegler-Nichols specifications, which involves determining the ultimate gain and the ultimate period of the plant. The resulting nonlinear gain functions can be rather complex and difficult to implement. In the absence of a nonlinear plant model extensive testing would be needed to

determine the ultimate gain and ultimate period before the controller could be designed.

In this thesis the basic nonlinear PID controller framework presented in Rugh(1987) is used. However, instead of using the Ziegler-Nichols tuning specifications to determine the controller gains, a simpler technique to determine the nonlinear gain functions is developed. This technique is then applied to several systems to determine how well this simplification works in practice. After reviewing the literature on other similar nonlinear control schemes, some conclusions will be presented.

CHAPTER 2

Non-Linear PID Controllers

Linear PID controllers are well known classical controllers that have been studied intensely for many years. However, with recent interest in modeling and controlling non-linear systems, the limitations of operating the non-linear system with a single linear controller have become readily apparent. Frequently the linear controller will operate well within a local family of set points but the global performance is not satisfactory. Global performance in this context means the ability to operate the system over a large range of set points in a narrow strip near the system equilibrium curve. The goal of this chapter is to describe a non-linear PID controller design scheme that attempts to improve global performance while maintaining the local operating properties of the linear controller.

The design process begins with a linearization of the non-linear plant. Several linearization techniques are known but the technique used here is a first order Taylor Series method (Wiberg, pp. 8-9). Consider a nth order plant model with equations of the form:

$$\dot{x}_1(t) = f_1(x_1(t),x_2(t),\ldots,x_n(t),u(t))$$

$$\dot{x}_2(t) = f_2(x_1(t),x_2(t),\ldots,x_n(t),u(t))$$

$$\vdots \qquad\qquad \vdots$$

$$\dot{x}_n(t) = f_n(x_1(t),x_2(t),\ldots,x_n(t),u(t)) \tag{2.1}$$

$$y(t) = f_{n+1}(x_1(t),x_2(t),\ldots,x_n(t),u(t)) \tag{2.2}$$

where i is any integer from 1 to n. Since the non-linear PID controller design is SISO, the plant family is limited to SISO plants. An equilibrium point is defined as follows:

$$0 = f_1(x_{1(eq)}, x_{2(eq)}, \ldots, x_{n(eq)}, u_{(eq)})$$

$$\begin{aligned} 0 &= f_2(x_{1(eq)}, x_{2(eq)}, \cdots, x_{n(eq)}, u_{(eq)}) \\ &\vdots \\ 0 &= f_n(x_{1(eq)}, x_{2(eq)}, \cdots, x_{n(eq)}, u_{(eq)}) \end{aligned} \tag{2.3}$$

$$y_{(eq)} = f_{n+1}(x_{1(eq)}, x_{2(eq)}, \ldots, x_{n(eq)}, u_{(eq)}) \tag{2.4}$$

With n + 1 equations and n + 2 unknowns there are an infinite number of solutions. The set of equilibrium points may be parametrized by the input $u_{(eq)}$. The plant can be linearized about any equilibrium point by the use of first order Taylor Series of the form:

$$\begin{aligned} \dot{x}_{\delta 1}(t) &= \sum_{j=1}^{n} \left[\Gamma_{1,j} \cdot x_{\delta j}(t) \right] + \Gamma_{1,u} \cdot u_{\delta}(t) \\ \dot{x}_{\delta 2}(t) &= \sum_{j=1}^{n} \left[\Gamma_{2,j} \cdot x_{\delta j}(t) \right] + \Gamma_{2,u} \cdot u_{\delta}(t) \\ &\vdots \\ \dot{x}_{\delta n}(t) &= \sum_{j=1}^{n} \left[\Gamma_{n,j} \cdot x_{\delta j}(t) \right] + \Gamma_{n,u} \cdot u_{\delta}(t) \end{aligned} \tag{2.5}$$

$$y_{\delta}(t) = \sum_{j=1}^{n} \left[\Gamma_{n+1,j} \cdot x_{\delta j}(t) \right] + \Gamma_{n+1,u} \cdot u_{\delta}(t) \tag{2.6}$$

$$\Gamma_{i,j} = \left[\frac{\partial f_i}{\partial x_j}\right]\Bigg|_{x_{1(eq)},x_{2(eq)},\ldots,x_{n(eq)},u_{(eq)}} \tag{2.7}$$

$$\Gamma_{i,u} = \left[\frac{\partial f_i}{\partial u}\right]\Bigg|_{x_{1(eq)},x_{2(eq)},\ldots,x_{n(eq)},u_{(eq)}} \tag{2.8}$$

where the delta indicates a deviation variable (e.g. $x_{\delta 2}(t) = x_2(t) - x_{2(eq)}$). These equations can be written in linear state space form:

$$\Delta\dot{x}(t) = \mathbb{A}_u \cdot \Delta x(t) + \mathbb{B}_u \cdot \Delta u(t) \tag{2.9}$$

$$\Delta y(t) = \mathbb{C}_u \cdot \Delta x(t) + \mathbb{D}_u \cdot \Delta u(t) \tag{2.10}$$

$$\mathbb{A}_u = \begin{bmatrix} \Gamma_{1,1} & \Gamma_{1,2} & \cdots & \Gamma_{1,n} \\ \Gamma_{2,1} & \Gamma_{2,2} & \cdots & \Gamma_{2,n} \\ \vdots & \vdots & \ddots & \vdots \\ \Gamma_{n,1} & \Gamma_{n,2} & \cdots & \Gamma_{n,n} \end{bmatrix} (n \times n) \tag{2.11}$$

$$\mathbb{B}_u = \begin{bmatrix} \Gamma_{1,u} \\ \Gamma_{2,u} \\ \vdots \\ \Gamma_{n,u} \end{bmatrix} (n \times 1), \quad \mathbb{C}_u = \begin{bmatrix} \Gamma_{n+1,1} \\ \Gamma_{n+1,2} \\ \vdots \\ \Gamma_{n+1,n} \end{bmatrix}^T (1 \times n) \tag{2.12-2.13}$$

$$\mathbb{D}_u = \begin{bmatrix} \Gamma_{n+1,u} \end{bmatrix} \tag{2.14}$$

$$\Delta\dot{x}(t) = \begin{bmatrix} \dot{x}_{\delta 1}(t) \\ \dot{x}_{\delta 2}(t) \\ \vdots \\ \dot{x}_{\delta n}(t) \end{bmatrix} (n \times 1) \tag{2.15}$$

$$\Delta x(t) = \begin{bmatrix} \dot{x}_{\delta 1}(t) \\ \dot{x}_{\delta 2}(t) \\ \vdots \\ \dot{x}_{\delta n}(t) \end{bmatrix} (n \times 1) \tag{2.16}$$

$$\Delta u(t) = u_{\delta}(t),\ \Delta y(t) = y_{\delta}(t) \tag{2.17-2.18}$$

where u indicates an association with a particular equilibrium point. Selection of an equilibrium operating point will result in unique $\mathbb{A}_u$, $\mathbb{B}_u$, $\mathbb{C}_u$, and $\mathbb{D}_u$ coefficient matrices that describe the plant dynamics in a local neighborhood near the selected equilibrium point. The eigenvalues of the $\mathbb{A}_u$ matrix can be analyzed for stability and a transfer function can be calculated in the following manner:

$$\mathbb{G}_u(s) = \mathbb{C}_u \cdot (s \cdot \mathbb{I}_n - \mathbb{A}_u)^{-1} \cdot \mathbb{B}_u + \mathbb{D}_u \tag{2.19}$$

where $\mathbb{I}_n$ is a n $\times$ n identity matrix and u indicates that the transfer function is associated with a particular equilibrium point. This process can be repeated for other equilibrium

points and stable regions of plant operation in the neighborhood of the equilibrium curve can be determined.

Normally, a single equilibrium point would be chosen and a single linear PID controller designed for operating the system. Ideally, in the case of a nonlinear PID controller all points along the plant equilibrium curve are used for designing a set of linear PID controllers. All points along the equilibrium curve would be used so that the exact character of the controller gain variations would be known. However, this would result in an infinite set of controllers so a finite set of equilibrium points are used and the resulting controller gain variations are approximated by the use of linear splines. Design performance characteristics are chosen that may vary with the equilibrium point and any available technique may be used to select the controller gains. This set of linear PID controllers will provide basis for a single non-linear PID controller whose linearization about each of these points gives the desired linear PID controller equation:

$$C_u(s) = K_1(u_{(eq)}) + \frac{K_2(u_{(eq)})}{s} + K_3(u_{(eq)})\cdot s \tag{2.20}$$

where u indicates that the controller transfer function is associated with a particular plant equilibrium point.

The gains from the set of linear PID controllers are used in a linear spline curve fitting technique (Gunzburger):

$$a \leq u(t) \leq b$$

$$K_i(u(t)) = \frac{K_i(a)}{b-a}\cdot(b - u(t)) + \frac{K_i(b)}{b-a}\cdot(u(t) - a)\ ,\ \ i = 1,\ldots,3 \tag{2.21}$$

where a and b are equilibrium control values from chosen set points. This is called gain-scheduling with respect to the plant input and allows the controller to alter gains such that the designed performance characteristics are maintained. Using the same non-linear PID controller state equations as in Rugh(1987), these non-linear functions are used in the PID controller state equations:

$$\dot{z}(t) = K_2[z(t)]\cdot e(t) \tag{2.22}$$

$$u(t) = z(t) + K_1[z(t)]\cdot e(t) + K_3[z(t)]\cdot \dot{e}(t) \tag{2.23}$$

where e(t) is the error between the command signal and the output of the plant. This controller at any closed-loop equilibrium point has the following properties: the error e(t) is zero and the controller state z(t) at equilibrium is equal to the equilibrium plant input.

As a verification, the controller state equations are linearized using first order Taylor Series with e(t) as the controller input and u(t) as the output:

$$f_1(z(t),e(t)) = K_2[z(t)]\cdot e(t) \tag{2.24}$$

$$f_2(z(t),e(t)) = z(t) + K_1[z(t)]\cdot e(t) + K_3[z(t)]\cdot \dot{e}(t) \tag{2.25}$$

$$e_{(eq)} = 0,\ \dot{e}_{(eq)} = 0,\ z_{(eq)} = u_{(eq)} \tag{2.26-2.28}$$

$$\dot{z}_\delta(t) = \left[\frac{\partial f_1}{\partial z}\right]_{z_{(eq)},e_{(eq)},\dot{e}_{(eq)}}\cdot z_\delta(t) + \left[\frac{\partial f_1}{\partial e}\right]_{z_{(eq)},e_{(eq)},\dot{e}_{(eq)}}\cdot e_\delta(t)$$

$$+ \left[\frac{\partial f_1}{\partial \dot{e}}\right]\Bigg|_{z_{(eq)},e_{(eq)},\dot{e}_{(eq)}} \cdot \dot{e}_\delta(t)$$

$$= K_2'(z_{(eq)})\cdot e_{(eq)}\cdot z_\delta(t) + K_2(z_{(eq)})\cdot e_\delta(t)$$

$$= K_2(u_{(eq)})\cdot e_\delta(t) \tag{2.29}$$

$$u_\delta(t) = \left[\frac{\partial f_2}{\partial z}\right]\Bigg|_{z_{(eq)},e_{(eq)},\dot{e}_{(eq)}} \cdot z_\delta(t) + \left[\frac{\partial f_2}{\partial e}\right]\Bigg|_{z_{(eq)},e_{(eq)},\dot{e}_{(eq)}} \cdot e_\delta(t)$$

$$+ \left[\frac{\partial f_2}{\partial \dot{e}}\right]\Bigg|_{z_{(eq)},e_{(eq)},\dot{e}_{(eq)}} \cdot \dot{e}_\delta(t)$$

$$= \left[1 + K_1'(z_{(eq)})\cdot e_{(eq)} + K_3'(z_{(eq)})\cdot \dot{e}_{(eq)}\right]\cdot z_\delta(t) + K_1(z_{(eq)})\cdot 1\cdot e_\delta(t)$$

$$+ K_3(z_{(eq)})\cdot \dot{e}_\delta(t)$$

$$= z_\delta(t) + K_1(u_{(eq)})\cdot e_\delta(t) + K_3(u_{(eq)})\cdot \dot{e}_\delta(t) \tag{2.30}$$

Converting these state equations to transfer function form (assuming the controller state initial condition is $u_{(eq)}$ and the error initial condition are both zero):

$$\mathbb{Z}_u(s) = \frac{K_2(u_{(eq)})}{s}\cdot \mathbb{E}_u(s) \tag{2.32}$$

$$\mathbb{U}_u(s) = \mathbb{Z}_u(s) + K_1(u_{(eq)})\cdot \mathbb{E}_u(s) + K_3(u_{(eq)})\cdot s\cdot \mathbb{E}_u(s)$$

$$= \frac{K_2(u_{(eq)})}{s} \cdot \mathbb{E}_u(s) + K_1(u_{(eq)}) \cdot \mathbb{E}_u(s) + K_3(u_{(eq)}) \cdot s \cdot \mathbb{E}_u(s) \tag{2.33}$$

$$\mathbb{C}_u(s) = \frac{\mathbb{U}_u(s)}{\mathbb{E}_u(s)} = K_1(u_{(eq)}) + \frac{K_2(u_{(eq)})}{s} + K_3(u_{(eq)}) \cdot s \tag{2.34}$$

which is the linearized form of the non-linear PID from equation 2.20.

CHAPTER 3

Control Of A Constant Volume, Non-Adiabatic, Continuously Stirred Tank Reactor

The details of the plant and the linear state feedback controller for this example are from Hoo and Kantor(1985). The process to be controlled is the chemical reaction within a constant volume, non-adiabatic, continuously stirred tank reactor (CSTR). This requires regulating reactor parameters so that a certain conversion rate from reactants to products is maintained. The model describing the CSTR is given by:

$$\dot{x}_1 = -x_1 + Da\cdot(1 - x_1)\cdot e^{\left[\frac{x_2}{1 + x_2/\gamma}\right]} \tag{3.1}$$

$$\dot{x}_2 = -x_2 + B\cdot Da\cdot(1 - x_1)\cdot e^{\left[\frac{x_2}{1 + x_2/\gamma}\right]} - u\cdot(x_2 - x_c) \tag{3.2}$$

where x_1 is the conversion, x_2 is the dimensionless temperature, u is the dimensionless heat transfer coefficient, x_c is the dimensionless cooling jacket temperature, Da is the Damkohler number, and B is the dimensionless heat of reaction. If $x_{2(eq)} = \alpha$ represents a desired equilibrium operating temperature for the CSTR then the equations for the equilibrium values of conversion and control are given by:

$$x_{1(eq)}(\alpha) = \frac{Da\cdot e^{\left[\frac{\alpha}{1 + \alpha/\gamma}\right]}}{1 + Da\cdot e^{\left[\frac{\alpha}{1 + \alpha/\gamma}\right]}} \tag{3.3}$$

$$u_{(eq)}(\alpha) = \frac{-\alpha + B \cdot x_{1(eq)}}{\alpha} \tag{3.4}$$

Figure 1 shows the reactor equilibrium curve (temperature vs. conversion) and Figure 2 shows the equilibrium values of the control with respect to α. The parameters of this CSTR model are given in Table 1. The dimensionless heat transfer coefficient u acts as the input to the plant and the dimensionless temperature x_2 acts as the output to the plant.

The equilibrium point $x_{1(eq)} = 0.5$, $x_{2(eq)} = 3$ was chosen as a reasonable operating point for the CSTR as it corresponds to moderate temperature and conversion. The linearized system at this equilibrium point is unstable and compensation is needed to operate the system in a stable manner.

Figure 3 shows a phase plot of the system operating with a linear state feedback controller. A linear controller was designed to place the eigenvalues of the closed-loop linearization about the operating point at -2. For initial conditions in the neighborhood of x $= [.1 \;\; 4]^T$, the system has transients with large overshoots in both temperature and conversion. The controller sends moderate initial control values to the plant when the initial state conditions are $x = [.1 \;\; 4]^T$ and $x = [.1 \;\; 5]^T$. The initial state and control values for the phase plot of Figure 3 are given in Table 2.

A linear PID was designed at the same equilibrium point as the state feedback controller. The plant is linearized using Taylor Series (see Chapter 2) and then modeled by:

$$\dot{x}_{\delta 1} = (-1 - Da \cdot \mu) \cdot x_{\delta 1} + \left[Da \cdot (1 - x_{1(eq)}) \cdot \mu \cdot \nu\right] \cdot x_{\delta 2} \tag{3.5}$$

$$\dot{x}_{\delta 2} = (-B \cdot Da \cdot \mu) \cdot x_{\delta 1} + \left[-1 + B \cdot Da \cdot (1 - x_{1(eq)}) \cdot \mu \cdot \nu - u_{eq}\right] \cdot x_{\delta 2}$$

$$+ (-\alpha + x_c)\cdot u_\delta \tag{3.6}$$

$$y_\delta = x_{\delta 2} \tag{3.7}$$

$$\mu = e^{\left[\frac{\alpha}{1 + \alpha/\gamma}\right]}, \quad \nu = \frac{1}{(1 + \alpha/\gamma)^2} \tag{3.8-3.9}$$

where delta indicates a deviation variable (e.g., $x_{\delta 2}(t) = x_2(t) - x_{2(eq)}$). Due to the difficulty of building an ideal differentiator a high-pass filter was used to approximate the differentiator. At low frequencies the high-pass filter resembles an ideal differentiator but at high frequencies it resembles a proportional gain. The linear controller transfer function is given by:

$$C(s) = K_1 + \frac{K_2}{s} + \frac{K_3\cdot s}{s + a}$$

$$= (K_1 + K_3) + \frac{K_2}{s} - \frac{a\cdot K_3}{s + a} \tag{3.10}$$

and leads to the state equations:

$$\dot{x}_1(t) = K_2\cdot e(t) \tag{3.11}$$

$$\dot{x}_2(t) = -a\cdot x_2(t) + a\cdot e(t) \tag{3.12}$$

$$u(t) = x_1(t) - K_3\cdot x_2(t) + (K_1 + K_3)\cdot e(t) \tag{3.13}$$

where a = 10 in this example. The transfer function of the linearized plant model at the equilibrium point $x_{1(eq)} = 0.5$, $x_{2(eq)} = 3$, $u_{(eq)} = 0.3333$ is:

$$G_u(s) = \frac{-3\cdot(s + 2)}{s^2 - 0.6552\cdot s - 1.3216} \tag{3.14}$$

with a zero at -2 and poles at 1.5232, -0.8679. The closed-loop performance characteristics chosen were a time constant of 0.3 s and 94.0% damping. A root locus design technique was used to calculate the controller gains and, after some gain adjustment, resulted in the following controller transfer function:

$$C(s) = -5 - \frac{6}{s} - \frac{2\cdot s}{s + 10} \tag{3.15}$$

The system with this controller transfer function has stable closed-loop poles (Figure 4) and adequate local performance characteristics
(Figure 5).

This example was intended to show that a system using a linear PID controller has good local performance but poor global performance. A nonlinear PID controller designed from a set of locally designed linear PID controllers would then show an improved global performance over a single linear PID controller. Simulations with this linear PID show that the system has reasonable performance over a wide range of initial conditions. However, the linear PID controller has superior performance to the system using the linear state feedback controller at certain initial conditions. Figure 6 shows a phase plot of the system with the linear PID controller, using the same initial conditions as the system with the linear state

feedback controller. Table 3 gives the initial state and control values for the phase plot of Figure 6. A comparison of Tables 2 and 3 will show that when the initial value of the dimensionless temperature x_2 deviates from the chosen operating value ($x_2 = 3$) the initial control value from the linear PID controller is much larger than the initial control value from the linear state feedback controller. The linear PID controller begins the simulation with zero initial conditions for its internal states. The initial control value is therefore a function of the initial error and the feedthrough term (due to the increased proportional gain caused by the differentiator approximation) from the linear PID controller. The larger initial control values in the region of initial conditions $x = [.1 \quad 4]^T$ force the linear PID controlled system towards the designed operating point more quickly than the linear state feedback controlled system, as can be seen from a comparison of Figures 3 and 6. However, the initial control values in the region of initial conditions $x = [.1 \quad 3]^T$ are lower for the linear PID controller than for the linear state feedback controller due to the low value of the initial error. The linear PID controlled system has to drift until the control is large enough to force the system towards the designed operating point. The linear state feedback controller uses moderate control values to move the system towards its designed operating point in a direct manner. Conclusion: dynamic output feedback may provide better performance at certain initial conditions than state feedback for non-linear systems.

Table 1. Parameters for CSTR Model used in Chapter 3

Dimensionless Cooling Jacket Temperature:	x_c	$= 0$
Damkohler Number:	Da	$= 0.05$
Dimensionless Heat of Reaction:	B	$= 8$
	γ	$= 2100$
Equilibrium Conversion:	x_1	$= 0.5$
Equilibrium Dimensionless Temperature:	x_2	$= 3$

Table 2. Initial State and Control Values for the Phase Plot of the Linear State Feedback Controlled System of Figure 3

$x_1 = 0.9$	$x_2 = 1$	$u = -3.8375$
$x_1 = 0.7$	$x_2 = 1$	$u = -3.3041$
$x_1 = 0.5$	$x_2 = 1$	$u = -2.7707$
$x_1 = 0.3$	$x_2 = 1$	$u = -2.2373$
$x_1 = 0.1$	$x_2 = 1$	$u = -1.7039$
$x_1 = 0.1$	$x_2 = 2$	$u = -0.1519$
$x_1 = 0.1$	$x_2 = 3$	$u = 1.4001$
$x_1 = 0.1$	$x_2 = 4$	$u = 2.9521$
$x_1 = 0.1$	$x_2 = 4.5$	$u = 3.7281$
$x_1 = 0.1$	$x_2 = 5$	$u = 4.5041$

Table 3. Initial State and Control Values for the Phase Plot of the Linear PID Controlled System of Figure 6

$x_1 = 0.9$	$x_2 = 1$	$u = -14$
$x_1 = 0.7$	$x_2 = 1$	$u = -14$
$x_1 = 0.5$	$x_2 = 1$	$u = -14$
$x_1 = 0.3$	$x_2 = 1$	$u = -14$
$x_1 = 0.1$	$x_2 = 1$	$u = -14$
$x_1 = 0.1$	$x_2 = 2$	$u = -7$
$x_1 = 0.1$	$x_2 = 3$	$u = 0$
$x_1 = 0.1$	$x_2 = 4$	$u = 7$
$x_1 = 0.1$	$x_2 = 4.5$	$u = 10.5$
$x_1 = 0.1$	$x_2 = 5$	$u = 14$

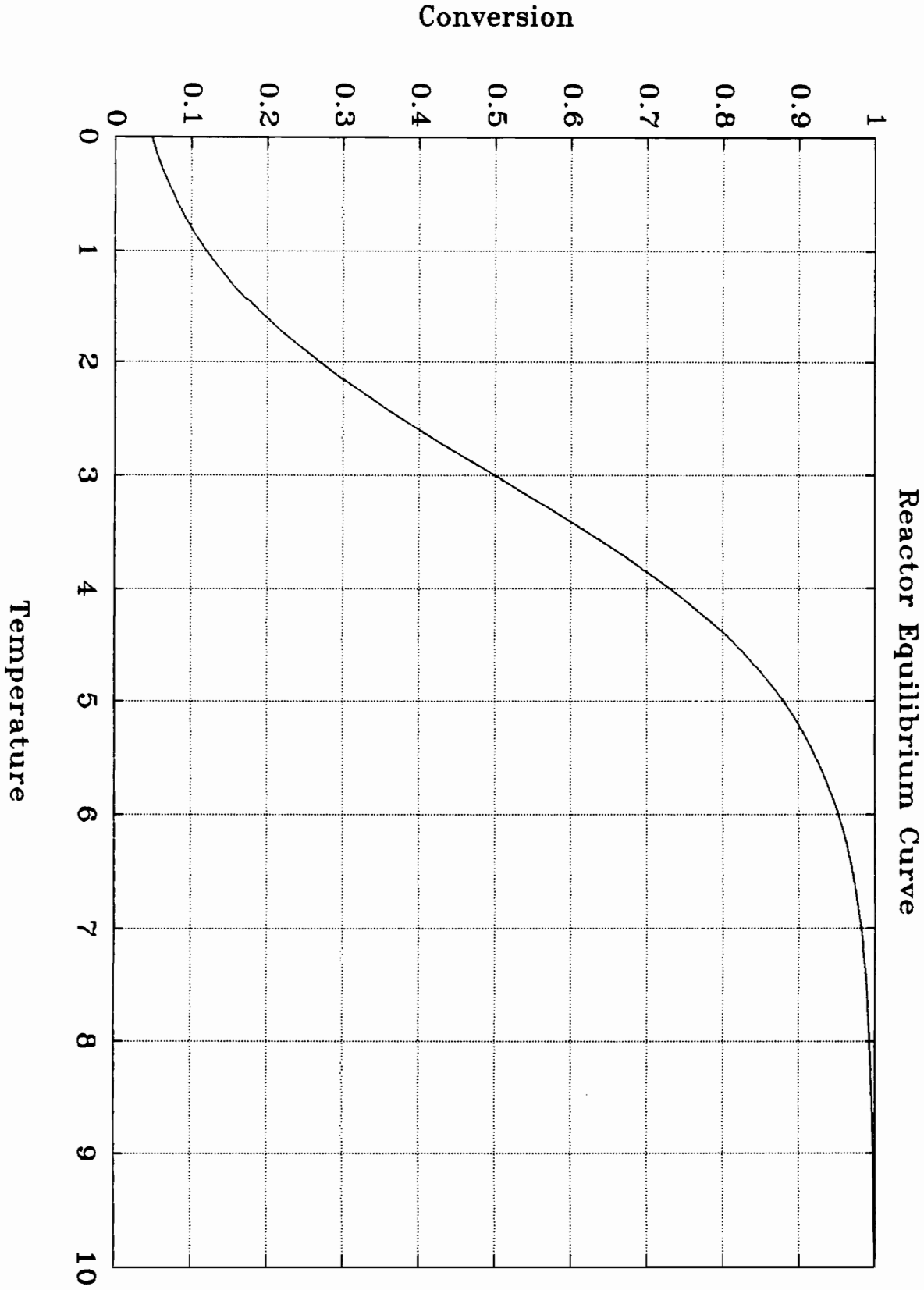
Reactor Equilibrium Curve
Conversion
1
0.9
0.8
0.7
0.6
0.5
0.4
0.3
0.2
0.1
0
0
1
2
3
4
5
6
7
8
9
10
Temperature

Figure 1

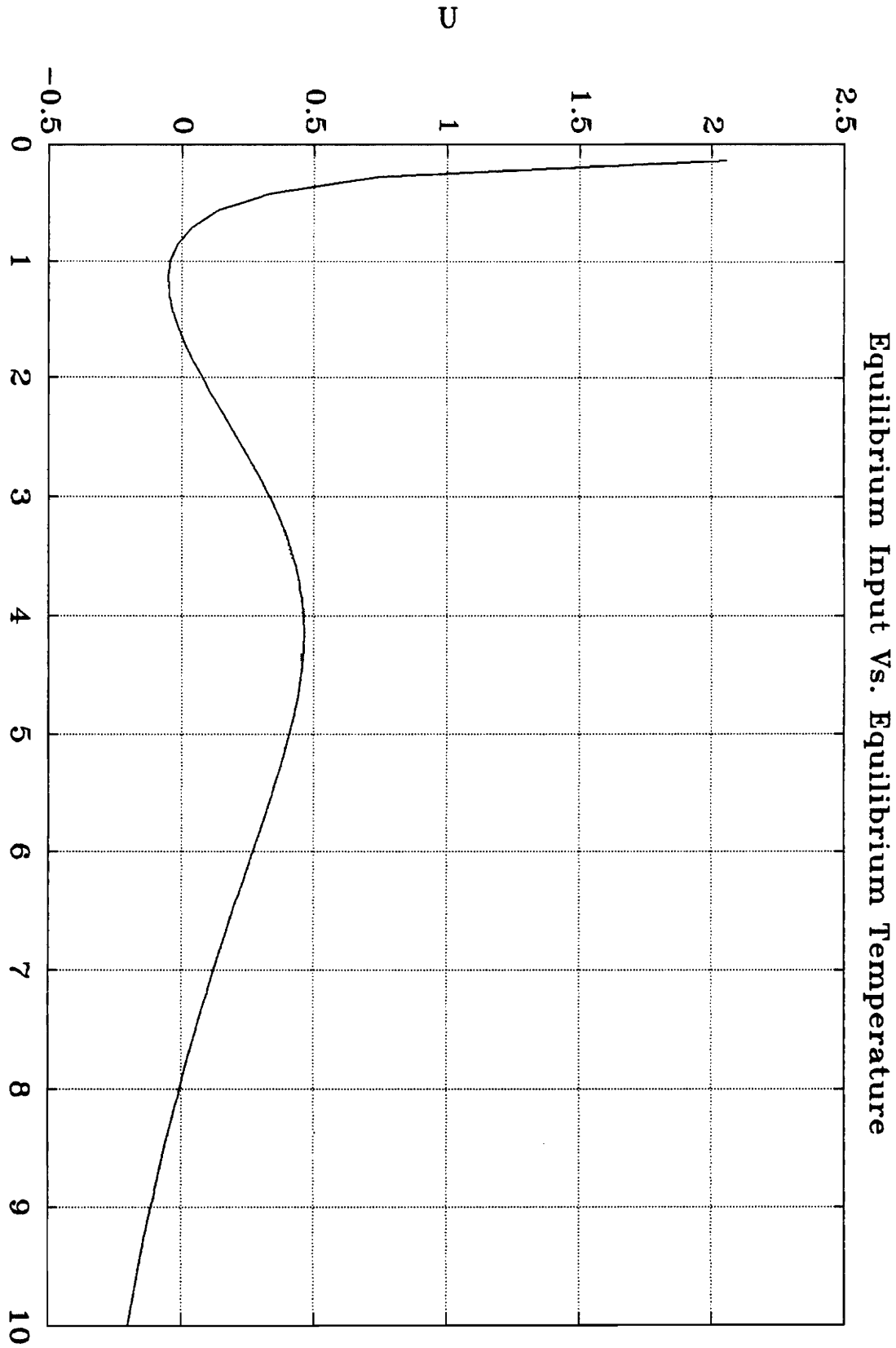
Equilibrium Input Vs. Equilibrium Temperature
U
2.5
2
1.5
1
0.5
0
−0.5
0
1
2
3
4
5
6
7
8
9
10
Temperature

Figure 2

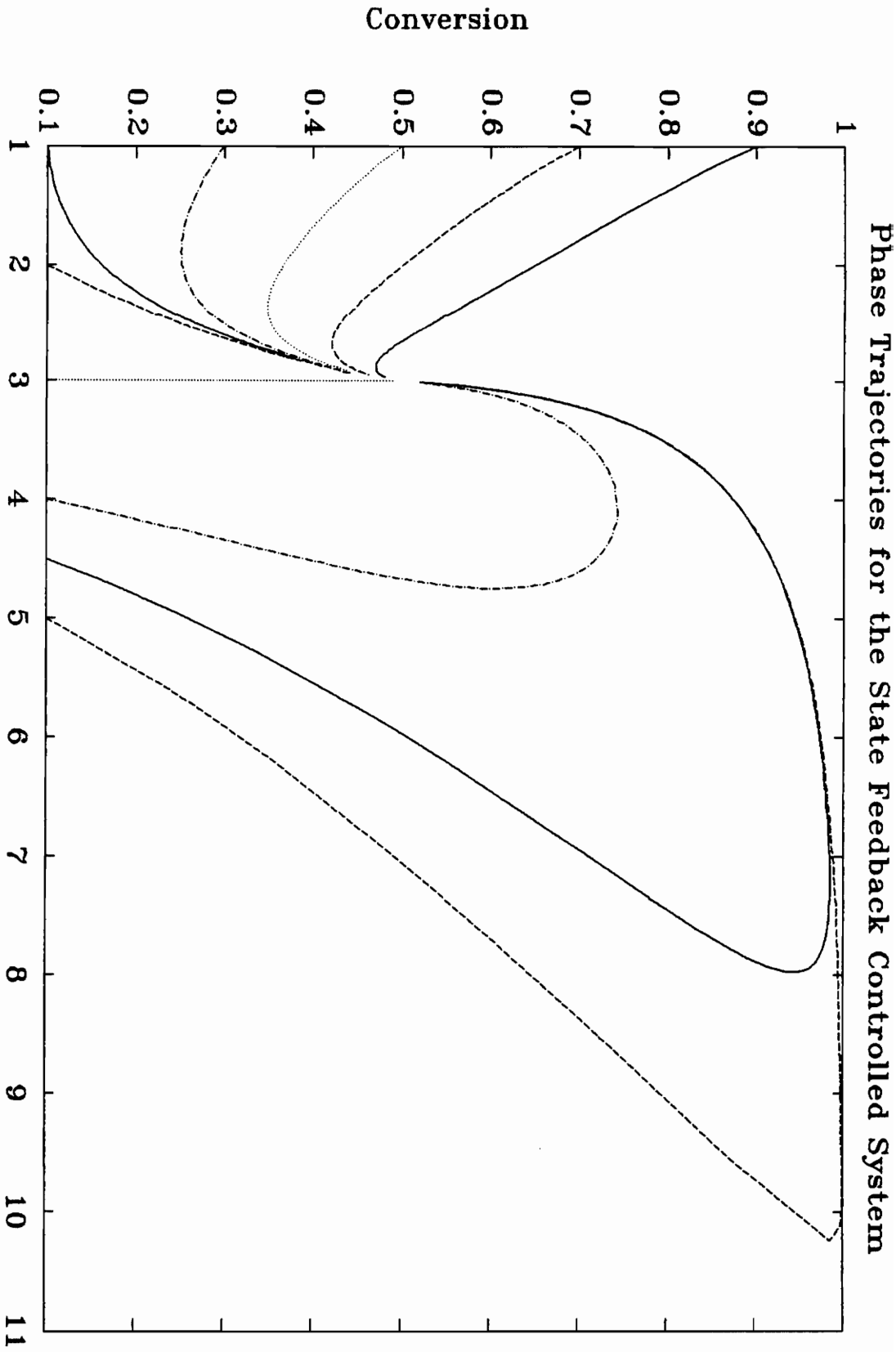
Phase Trajectories for the State Feedback Controlled System
Conversion
1
0.9
0.8
0.7
0.6
0.5
0.4
0.3
0.2
0.1
1
2
3
4
5
6
7
8
9
10
11
Temperature

Figure 3

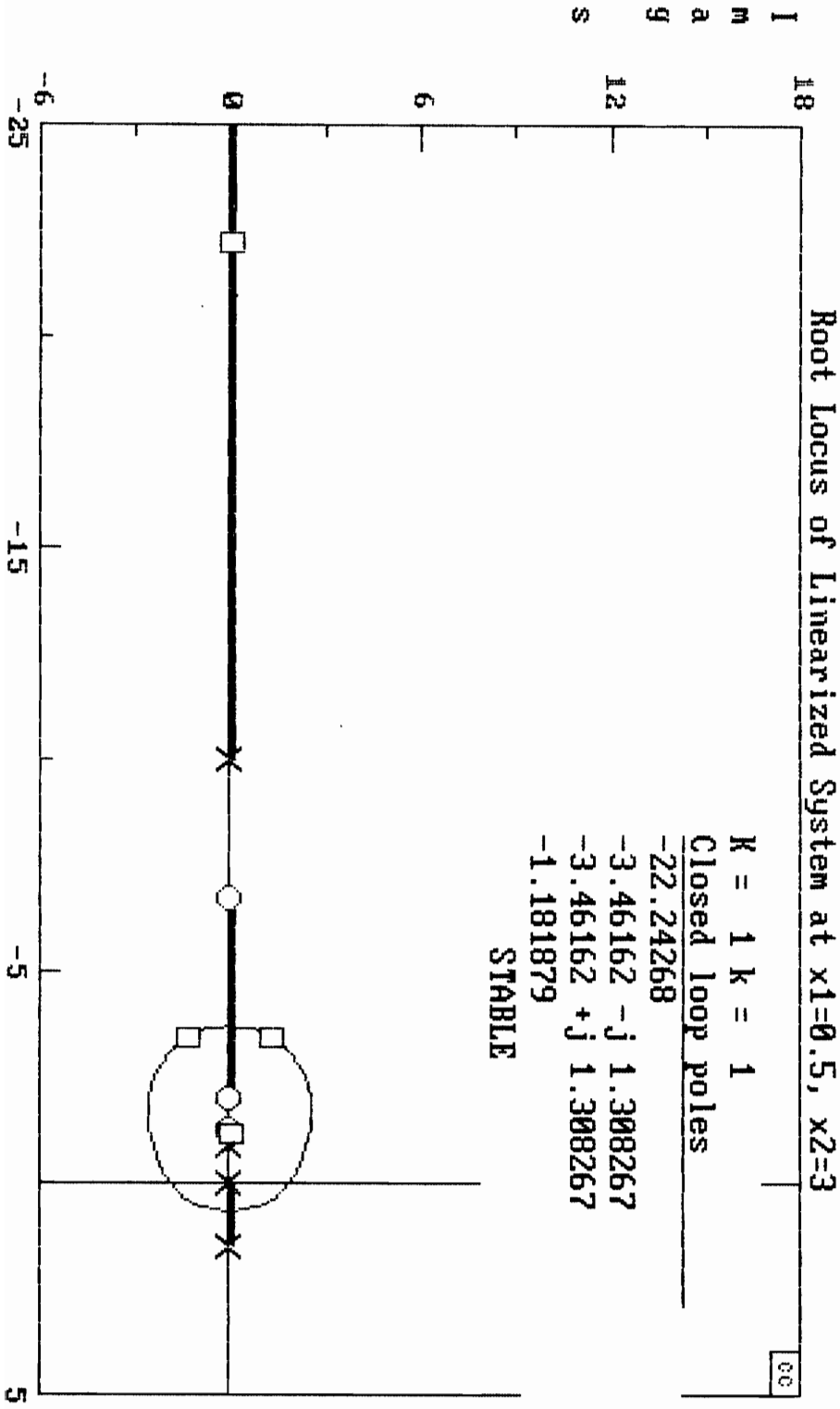
Root Locus of Linearized System at x1=0.5, x2=3
K = 1 k = 1
Closed loop poles
-22.24268
-3.46162 -j 1.308267
-3.46162 +j 1.308267
-1.181879
STABLE
Imag
18
12
6
0
-6
-25
-15
-5
5

Figure 4

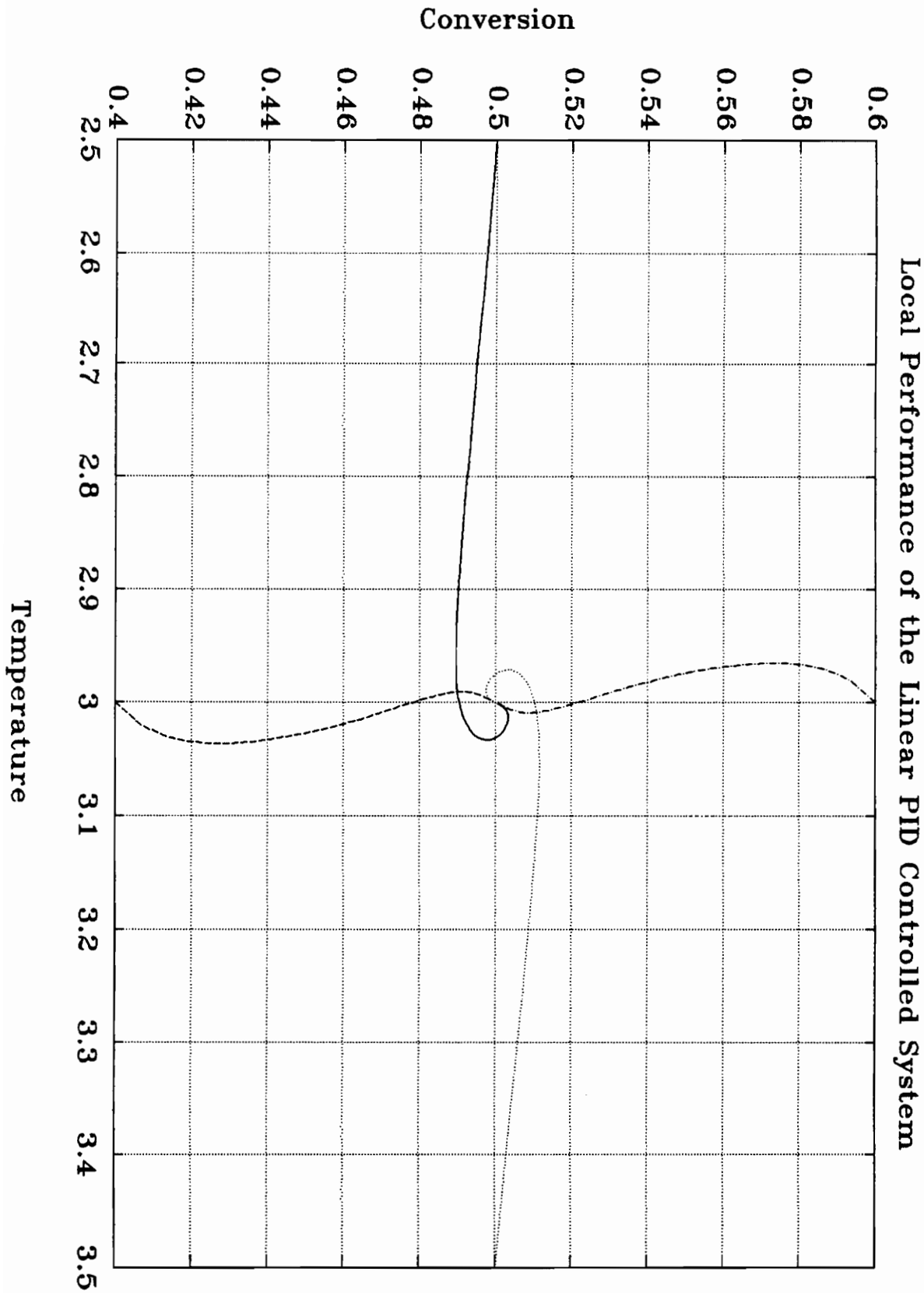
Local Performance of the Linear PID Controlled System
Conversion
0.6
0.58
0.56
0.54
0.52
0.5
0.48
0.46
0.44
0.42
0.4
2.5
2.6
2.7
2.8
2.9
3
3.1
3.2
3.3
3.4
3.5
Temperature

Figure 5

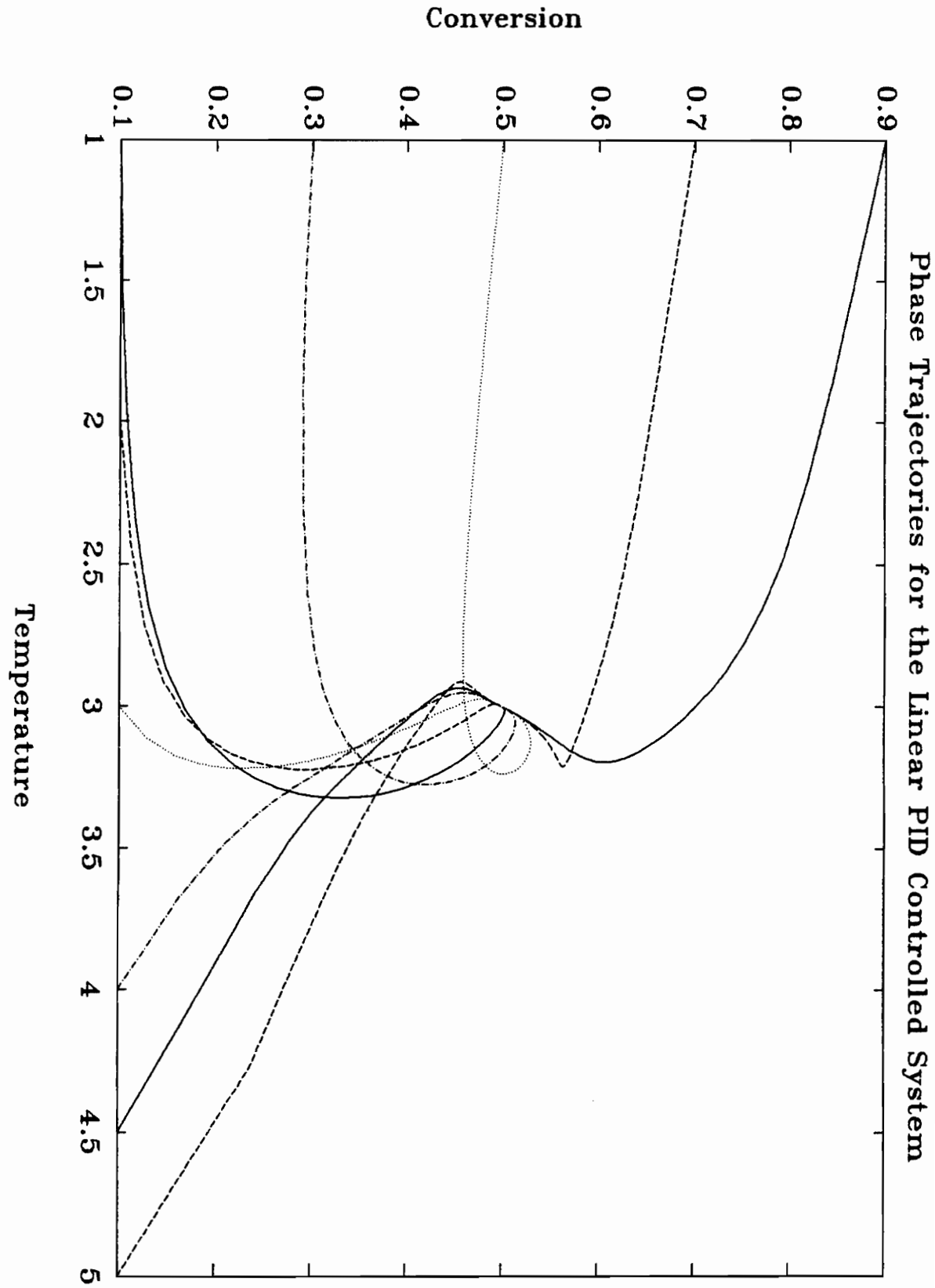
Phase Trajectories for the Linear PID Controlled System
Conversion
0.9
0.8
0.7
0.6
0.5
0.4
0.3
0.2
0.1
1
1.5
2
2.5
3
3.5
4
4.5
5
Temperature

Figure 6

CHAPTER 4

Control Of An Ideal Continuously Stirred Tank Reactor

The details of the plant and the linear controller for this example are from Economou, Morari and Palsson (1986). The process to be controlled is a reversible exothermic reaction conducted within an ideal continuously stirred tank reactor (CSTR). The chemical equation describing the reaction is given by:

$$A \underset{k_{-1}}{\overset{k_1}{\rightleftharpoons}} R \tag{4.1}$$

and the model describing the CSTR is given by:

$$\dot{A}_o = \frac{1}{\tau}\cdot(A_i - A_o) - k_1(T_o)\cdot A_o + k_{-1}(T_o)\cdot R_o \tag{4.2}$$

$$\dot{R}_o = \frac{1}{\tau}\cdot(R_i - R_o) + k_1(T_o)\cdot A_o - k_{-1}(T_o)\cdot R_o \tag{4.3}$$

$$\dot{T}_o = \frac{-\Delta H_R}{\rho\cdot C_p}\cdot(k_1(T_o)\cdot A_o - k_{-1}(T_o)\cdot R_o) + \frac{1}{\tau}\cdot(T_i - T_o) \tag{4.4}$$

$$k_1(T_o) = C_1\cdot\exp\left[\frac{-Q_1}{\mathcal{R}\cdot T_o}\right],\ k_{-1}(T_o) = C_{-1}\cdot\exp\left[\frac{-Q_{-1}}{\mathcal{R}\cdot T_o}\right] \tag{4.5-4.6}$$

The parameters and the desired equilibrium operating point are given in Table 4. The control objective is to operate the system near the equilibrium peak point to

maximize the output product concentration while maintaining closed-loop stability. The input temperature T_i acts as the input to the plant and the output product concentration R_o acts as the output to the plant.

The reactor equilibrium curve (Figure 7) was obtained by setting the state equations equal to zero and solving for A_o, R_o, T_o and T_i. A maximum point occurs in the curve at a output temperature of 438.5° K and an output product concentration of 0.5088 mol/l. According to Economou, Morari and Palsson (1986):

> Note that because of the conversion maximum, the system gain changes sign as the operating point changes from one side of the maximum to the other. Systems of this type are not "integral controllable"; i.e., they *cannot be stable* over the entire operating region when controllers with integral action are employed.

The solution that Economou, Morari and Palsson (1986) recommends for the linear controller is the removal of the "no offset requirement" (i.e. remove the integrator). This allows the possibility of a stable linear controller over the entire region of interest. The type of controller they used is a simple proportional controller with a gain of 1500.

The solution offered by the nonlinear PID controller presented here allows integral control to operate over the entire region. The controller gains are scheduled to change sign when the plant changes sign, permitting stability for the system. One of the potential drawbacks to this technique is synchronizing the change in sign of the plant and the controller. If the actual peak of the equilibrium curve differs significantly from the calculated peak undesirable dynamics could occur.

Six points along the equilibrium curve were chosen as design points for the set of linear PIDs. These points are shown in Figure 7 as small x's and are given in Table 5. A point was not chosen at the peak of the equilibrium curve due to the linearized system having zero steady state gain at this point. The desired performance characteristics of the closed-loop system were chosen as a time constant of 50 s and 70.7% damping. A root locus design technique utilized a linearized model of the plant about each equilibrium point. The linearized plant is modeled by:

$$x_1(t) = A_o, \;\; x_2(t) = R_o, \;\; x_3(t) = T_o \tag{4.7-4.9}$$

$$\mu = \frac{Q_1}{\mathfrak{R}\cdot(T_{o(eq)})^2}, \; \nu = \frac{-\Delta H_R}{\rho\cdot C_p} \tag{4.10-4.11}$$

$$\begin{aligned}\dot{x}_{\delta 1}(t) = &\left[-\tfrac{1}{\gamma} - k_1(T_{o(eq)})\right]\cdot x_{\delta 1}(t) + \left[k_{-1}(T_{o(eq)})\right]\cdot x_{\delta 2}(t) \\ &+ \left[-k_1(T_{o(eq)})\cdot A_{o(eq)}\cdot\mu + k_{-1}(T_{o(eq)})\cdot R_{o(eq)}\cdot\mu\right]\cdot x_{\delta 3}(t)\end{aligned} \tag{4.12}$$

$$\begin{aligned}\dot{x}_{\delta 2}(t) = &\left[k_1(T_{o(eq)})\right]\cdot x_{\delta 1}(t) + \left[-\tfrac{1}{\gamma} - k_{-1}(T_{o(eq)})\right]\cdot x_{\delta 2}(t) \\ &+ \left[k_1(T_{o(eq)})\cdot A_{o(eq)}\cdot\mu - k_{-1}(T_{o(eq)})\cdot R_{o(eq)}\cdot\mu\right]\cdot x_{\delta 3}(t)\end{aligned} \tag{4.13}$$

$$\begin{aligned}\dot{x}_{\delta 3}(t) = &\left[\nu\cdot k_1(T_{o(eq)})\right]\cdot x_{\delta 1}(t) + \left[-\nu\cdot k_{-1}(T_{o(eq)})\right]\cdot x_{\delta 2}(t) \\ &+ \left[\nu\cdot\left[k_1(T_{o(eq)})\cdot A_{o(eq)}\cdot\mu - k_{-1}(T_{o(eq)})\cdot R_{o(eq)}\cdot\mu\right] - \tfrac{1}{\gamma}\right]\cdot x_{\delta 3}(t)\end{aligned}$$

$$+ \left[\frac{1}{\tau}\right]\cdot u_\delta(t) \tag{4.14}$$

$$y_\delta(t) = x_{\delta 2}(t) \tag{4.15}$$

where delta indicates a deviation variable (e.g., $x_{\delta 2}(t) = x_2(t) - x_{2(eq)}$) from the Taylor Series used to form this linearized model. Due to the difficulty of modeling an ideal differentiator a high-pass filter was used to approximate the differentiator. The linearized controller transfer function is given by:

$$\begin{aligned} \mathbf{C_u}(s) &= K_1(u_{(eq)}) + \frac{K_2(u_{(eq)})}{s} + \frac{K_3(u_{(eq)})\cdot s}{s + a} \\ &= (K_1(u_{(eq)}) + K_3(u_{(eq)})) + \frac{K_2(u_{(eq)})}{s} - \frac{a\cdot K_3(u_{(eq)})}{s + a} \\ &= \frac{(K_1(u_{(eq)}) + K_3(u_{(eq)}))\cdot s^2 + (a\cdot K_1(u_{(eq)}) + K_2(u_{(eq)}))\cdot s + a\cdot K_2(u_{(eq)})}{s^2 + a\cdot s} \end{aligned} \tag{4.16}$$

which results in the state space equations:

$$\dot{x}_1(t) = K_2\left[x_1(t)\right]\cdot e(t) \tag{4.17}$$

$$\dot{x}_2(t) = -ax_2 + ae(t) \tag{4.18}$$

$$u(t) = x_1(t) - K_3\left[x_1(t)\right]\cdot x_2(t) + \left[K_1\left[x_1(t)\right] + K_3\left[x_1(t)\right]\right]\cdot e(t) \tag{4.19}$$

where $a = 1$ in this example. At any closed-loop equilibrium point this controller has the

following properties: $x_1(t) = u_{(eq)}$, $x_2(t) = 0$, and $e(t) = 0$. The non-linear controller was constructed by interpolating the gains at each chosen equilibrium point (given in Table 6) using linear spline equations of the form (Gunzburger):

$$c \leq u(t) < d$$

$$K_i(u(t)) = \frac{(d - u(t))}{d - c} \cdot K_i(c) + \frac{(u(t) - c)}{d - c} \cdot K_i(d) \tag{4.20}$$

where $i = 1,\ldots,3$ represents the gain associated with each element of the PID. Substituting $x_1(t)$ for $u(t)$ leads to the state space model of the non-linear PID controller as described by equations 4.17-4.19.

As an example of the design process, the calculation of the controller at one of the chosen equilibrium points is detailed. At the equilibrium point with output temperature $T_o = 377.5$ °K, output product concentration $R_o = 0.3022$ mol/l, output reactant concentration $A_o = 0.6978$ mol/l, and input temperature $T_i = 376.0$ °K, the linearized plant transfer function is:

$$G_u = \frac{2.780\times10^{-6}\cdot s + 4.634\times10^{-8}}{s^3 + 5.934\times10^{-2}\cdot s^2 + 1.145\times10^{-3}\cdot s + 7.225\times10^{-6}} \tag{4.21}$$

with a zero at -1.667×10^{-2}, and poles at -2.592×10^{-2}, -1.742×10^{-2}, and -1.600×10^{-2}. To obtain closed-loop system dynamics of a 50 s time constant and 70.7% damping, the root locus plot of the closed-loop system must pass through the point $-0.02 + j\cdot0.02$. From classical control theory the following equation is true of all root locus plots (Biernson, pp. 495-497):

$$\sum_{i=1}^{m} \angle z_i - \sum_{j=1}^{n} \angle p_j = \pm k \cdot 180^\circ \tag{4.22}$$

where $\angle z_i$ is the angle of a line drawn from a chosen point in the root locus plane to a open-loop zero, $\angle p_j$ is the angle of a line drawn from the same chosen point in the root locus plane to a open-loop pole, m is the number of open-loop zeros, n is the number of open-loop poles, and k is any arbitrary integer. Since the controller poles are known to be 0 and -1, the sum of the angles of the controller zeros can be calculated using equation 4.22:

$$z_1 = -0.01667,\ p_1 = -0.02592,\ p_2 = -0.01742 \tag{4.23-4.25}$$

$$p_3 = -0.01600,\ p_4 = 0,\ p_5 = -1 \tag{4.26-4.28}$$

$$\angle z_1 = \text{Arctan}\left[\frac{-0.02}{-0.01667 + 0.02}\right] = -80.55^\circ \tag{4.29}$$

$$\angle p_1 = \text{Arctan}\left[\frac{-0.02}{-0.02601 + 0.02}\right] = -106.5^\circ \tag{4.30}$$

$$\angle p_2 = \text{Arctan}\left[\frac{-0.02}{-0.01667 + 0.02}\right] = -82.65^\circ \tag{4.31}$$

$$\angle p_3 = \text{Arctan}\left[\frac{-0.02}{-0.01667 + 0.02}\right] = -78.69^\circ \tag{4.32}$$

$$\angle p_4 = \text{Arctan}\left[\frac{-0.02}{0 + 0.02}\right] = -45.00^\circ \tag{4.33}$$

$$\angle p_5 = \text{Arctan}\left[\frac{-0.02}{-1 + 0.02}\right] = -178.8^\circ \tag{4.34}$$

$$\angle z_1 - \angle p_1 - \angle p_2 - \angle p_3 - \angle p_4 - \angle p_5 = 411.1^\circ = 231.1^\circ + 180.0^\circ \tag{4.35}$$

$$\angle z_2 + \angle z_3 = -231.1^\circ \tag{4.36}$$

For simplicity, the controller will have a double zero on the real axis in the root locus plane:

$$\angle z_2 = \angle z_3 = -115.6^\circ \tag{4.37}$$

$$-115.6^\circ = \text{Arctan}\left[\frac{-0.02}{\alpha + 0.02}\right] \tag{4.38}$$

$$\alpha = \left[\frac{-0.02}{\tan(-115.6^\circ)}\right] - 0.02 = -0.02956 \tag{4.39}$$

This results in the linearized controller transfer function:

$$\begin{aligned} C_u(s) &= \frac{K_c \cdot (s + 2.956\times10^{-2})^2}{s\cdot(s + 1)} \\ &= \frac{K_c \cdot (s^2 + 5.913\times10^{-2}\cdot s + 8.741\times10^{-4})}{s^2 + s} \end{aligned} \tag{4.40}$$

where K_c is the controller transfer gain required to force one of the closed-loop system poles to be $-0.02 + j\cdot0.02$. Figure 8 shows a root locus analysis of the system with $K_c = 8585$ and the resulting closed-loop poles. Comparing equation 4.40 with equation 4.16 results in the following values of the controller gains:

$$K_2(u_{(eq)}) = \frac{K_c \cdot 8.741 \times 10^{-4}}{a} = 7.504 \tag{4.41}$$

$$K_1(u_{(eq)}) = \frac{K_c \cdot 5.913 \times 10^{-2} - K_2(u_{(eq)})}{a} = 500.1 \tag{4.42}$$

$$K_3(u_{(eq)}) = K_c - K_1(u_{(eq)}) = 8085 \tag{4.43}$$

These controller gains (along with the controller gains from the other five linear PID designs) are used in the linear spline equations to form the nonlinear PID gains. Plots of these gains with respect to T_i are shown in Figures 9-11.

With this type of controller, good performance is expected with regard to small state disturbances due to the design. The error associated with linear splines is bounded by (Gunzburger):

$$|\text{error}| \leq \frac{\left\| \mathcal{K}_i''(u(t)) \right\|_\infty \cdot (d - c)^2}{8} \tag{4.44}$$

where $\mathcal{K}$ is the true nonlinear gain function and $i = 1,\ldots,3$ represents the gain associated with each element of the PID. The maximum bound for the error occurs between two inflection points and, after examining plots of the nonlinear gain functions, the system response to small state disturbances near the equilibrium point $R_o = 0.4800$ mol/l, $T_o = 468.4$ °K was observed. This particular point was chosen because it appeared to be between two inflection points and, therefore, some error in the linear spline functions is possible. As can be seen from Figure 12, when the system operates under an output temperature disturbance, the output product concentration adjusts quickly to the new output temperature. When the system moves back to the commanded operating point, overshoots

in temperature and concentration occur. When the system operates under an output product concentration disturbance, the temperature will begin to change and then the system corrects itself and moves back to the commanded operating point with no overshoot.

In the study of CSTR operation, there are several operating conditions that have particular interest. One of these operating conditions is startup performance. If startup performance is poor then safety restrictions could be exceeded or a loss of reactor efficiency could occur. The reactor startup was simulated with the following initial conditions: output product concentration $R_o = 0$ mol/l, output reactant concentration $A_o = 1.0$ mol/l, output temperature 330.0 °K, input temperature 330.0 °K, and the controller initial state x $= [330.0 \;\; 0]^T$. A first-order exponential filter with a 60 s time constant was used to smooth the step changes in command signal. Figure 13 shows the input response of the reactor. The large variation of the input temperature T_i in the first minute of the simulation is due to the initial condition of the second controller state (the one that approximates the differentiator). With a change in the command signal there is a large variation of the second controller state (Figure 14) and this causes the variation of input temperature T_i. A lower bandwidth command signal filter might reduce the initial command signal rate of change and thereby reduce the large variation in the second controller state that affects the input temperature response. Figure 15 shows that the variation of the input temperature T_i affects the smoothness of the output temperature T_o. Figure 16 shows that the output product concentration R_o moves smoothly from its initial value to its final value of 0.5080 mol/l. Figure 17 shows a phase plot of output temperature T_o versus output product concentration R_o. The system has a smooth transition to the desired operating point even with the large variation of input temperature T_i. Figure 18 shows the output of the first controller state.

Another CSTR operating condition worth investigating is system performance with

regard to parameter variations. A realistic variation is a disturbance in the input reactant concentration A_i. Simulations of the system operating near the peak equilibrium point with a -2% input reactant concentration disturbance (A_i) show that the nonlinear PID controller has definite advantages over the linear controller. The disturbance forces a downward shift in the equilibrium curve (due to the reduction of input reactant concentration A_i (Figure 19) and the system can never approach the commanded conversion rate. The desired control strategy is to operate the system at the maximum conversion rate until the disturbance is removed. The linear controller forces the system to a higher operating temperature until the commanded value of the output product concentration is met. However, this forces the system beyond the peak equilibrium point and the system becomes unstable. Figure 20 shows how the input temperature T_i climbs dramatically after the system crosses the peak of the equilibrium curve (T_i at the peak is 436.0 °K). Figure 21 shows the output temperature T_o increasing exponentially after crossing the peak equilibrium point. Figure 22 shows the output response and how the output product concentration R_o decreases exponentially in response to the input temperature T_i. Figure 23 is a phase plot of output temperature T_o versus output product concentration R_o. This shows that the system is increasing the output temperature in an vain attempt to increase the output product concentration. Since the system is operating on the right side of the peak equilibrium point, this has the effect of decreasing the output product concentration and, hence, the system is now unstable. The nonlinear controller operates the system at the peak equilibrium point of the shifted equilibrium curve ($R_o = 0.4986$ mol/l, $T_o = 438.5$ °K) to maximize the conversion rate. At this point the gains of the controller approach zero and the system continues to operate in a stable manner. However, when the disturbance is turned off (after 20 minutes), the system is extremely slow in returning to its

previous operating point. Figure 24 shows the input response and how the input temperature T_i levels off when it approaches the peak equilibrium point. When the disturbance is turned off, the input temperature slowly drops as the system begins to return to its equilibrium value. Figure 25 shows how the output temperature T_o also levels off at the peak equilibrium point, and slowly drops towards its previous point. Figure 26 shows the output response and how, after the disturbance is turned off, the output product concentration R_o returns to the peak equilibrium value. Figure 27 is a phase plot of output temperature versus output product concentration. This plot shows the system moving smoothly to the peak of the shifted equilibrium curve and hardly moving when the disturbance is turned off. Figures 28 and 29 show the responses of the controller states.

Comparison of the nonlinear PID controller performance with the performance of the computationally complex nonlinear IMC controller performance described in Economou, Morari, and Palsson (1986) shows some favorable results. The phase plots of the two systems under startup conditions are somewhat similar, but the nonlinear PID controlled system initially has a more rapid increase in output temperature T_o than the nonlinear IMC controlled system. When the CSTR is operating under the -2% input reactant disturbance A_i the plots of output product concentration R_o and input temperature T_i are remarkably similar. However, when the disturbance is turned off the nonlinear IMC controller moves the system back to the previous operating point more rapidly than the nonlinear PID controller.

Improving the performance of the nonlinear PID controlled system after the disturbance is turned off poses some problems. Letting the gains go to zero at the peak of the equilibrium curve removes any control over the system at this point. In order to return to controlled operation the system must move away from the peak equilibrium point. However, as in the case of the input reactant concentration disturbance, the controller is

forcing the system to operate at the peak equilibrium point. This raises the question of whether one or more of the controller gains should be nonzero at or near the peak equilibrium point. A nonzero gain in this region could cause undesired system dynamics or even instability. Further study of this type of controller could address this problem and possibly find a solution.

Table 4. Parameters for the CSTR Model used in Chapter 4

Flow Rate per Unit Volume	$\tau = 60$ s
Forward Rate Constant	$C_1 = 5 \times 10^3\ s^{-1}$
Reverse Rate Constant	$C_{-1} = 1 \times 10^6\ s^{-1}$
Forward Activation Energy	$Q_1 = 10\ 000$ cal/mol
Reverse Activation Energy	$Q_{-1} = 15\ 000$ cal/mol
Ideal Gas Constant	$\mathfrak{R} = 1.987$ cal/mol·°K
Heat of Reaction	$-\Delta H_R = 5000$ cal/mol
Density	$\rho = 1$ kg/l
Heat Capacity	$C_p = 1000$ cal/kg·°K
Input Reactant Concentration	$A_i = 1.0$ mol/l
Output Reactant Concentration	$A_o = 0.4920$ mol/l
Input Product Concentration	$R_i = 0.0$ mol/l
Output Product Concentration	$R_o = 0.5080$ mol/l
Input Stream Temperature	$T_i = 432.0$°K
Output Stream Temperature	$T_o = 434.5$°K

Table 5. Six Points from the Reactor Equilibrium Curve used to Design the Nonlinear PID

Point 1	$R_o = 0.0492$ mol/l	$T_o = 323.2^\circ K$	$u_{(eq)} = 323.0^\circ K$
Point 2	$R_o = 0.3022$ mol/l	$T_o = 377.5^\circ K$	$u_{(eq)} = 376.0^\circ K$
Point 3	$R_o = 0.4602$ mol/l	$T_o = 408.3^\circ K$	$u_{(eq)} = 406.0^\circ K$
Point 4	$R_o = 0.4800$ mol/l	$T_o = 468.4^\circ K$	$u_{(eq)} = 466.0^\circ K$
Point 5	$R_o = 0.3008$ mol/l	$T_o = 563.5^\circ K$	$u_{(eq)} = 562.0^\circ K$
Point 6	$R_o = 0.1999$ mol/l	$T_o = 643.0^\circ K$	$u_{(eq)} = 642.0^\circ K$

Table 6. Gains of the Set of Linear PIDs Corresponding to the Six Points in Table 5

Point 1	$K_1 = 200.3$	$K_2 = 25.14$	$K_3 = 3.889\times10^4$
Point 2	$K_1 = 500.1$	$K_2 = 7.504$	$K_3 = 8085$
Point 3	$K_1 = 675.1$	$K_2 = 13.56$	$K_3 = 8069$
Point 4	$K_1 = -1290$	$K_2 = -35.69$	$K_3 = -1.102\times10^4$
Point 5	$K_1 = -1293$	$K_2 = -38.24$	$K_3 = -1.028\times10^4$
Point 6	$K_1 = -2144$	$K_2 = -63.83$	$K_3 = -1.696\times10^4$

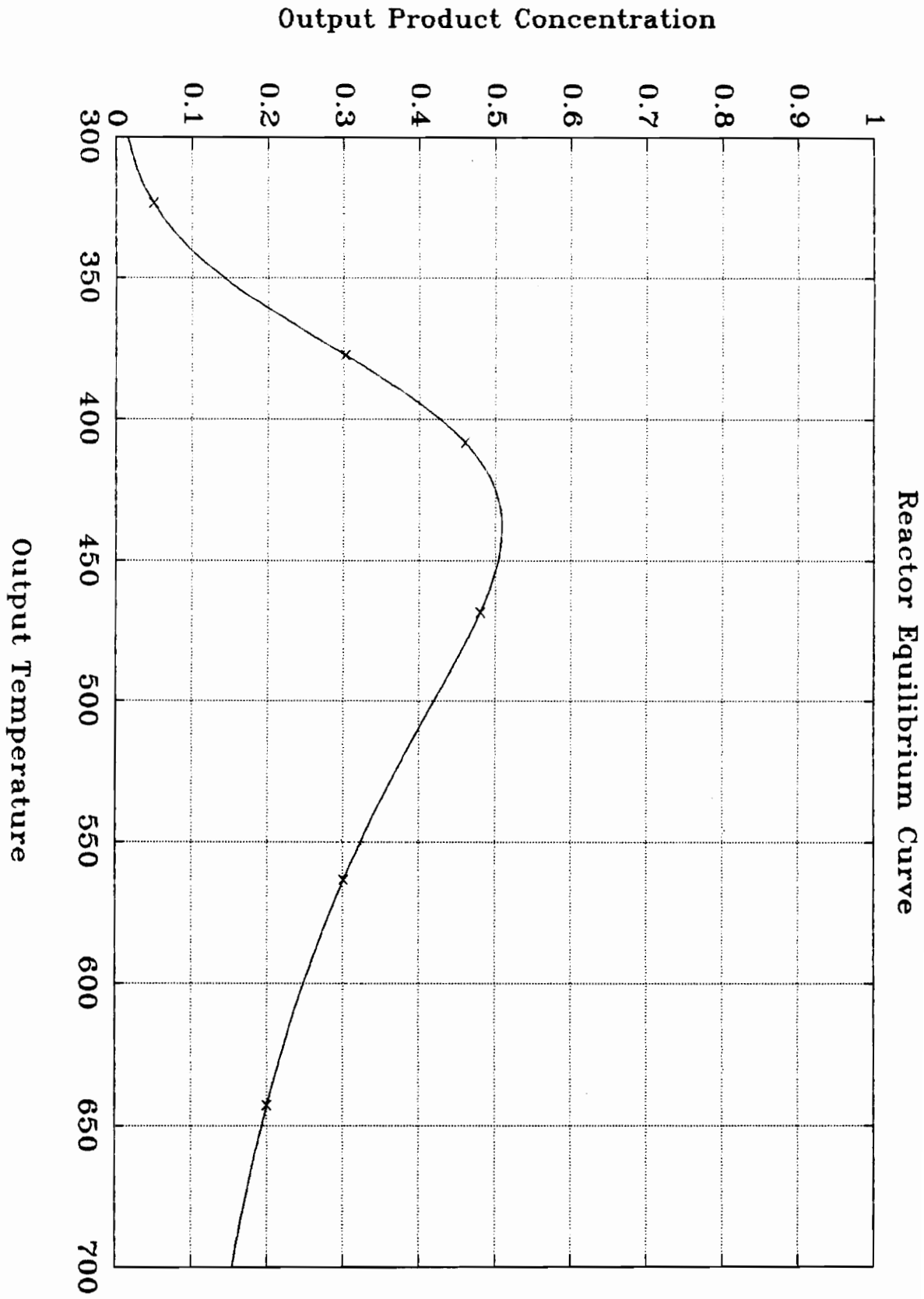
Reactor Equilibrium Curve
Output Product Concentration
1
0.9
0.8
0.7
0.6
0.5
0.4
0.3
0.2
0.1
0
300
350
400
450
500
550
600
650
700
Output Temperature

Figure 7

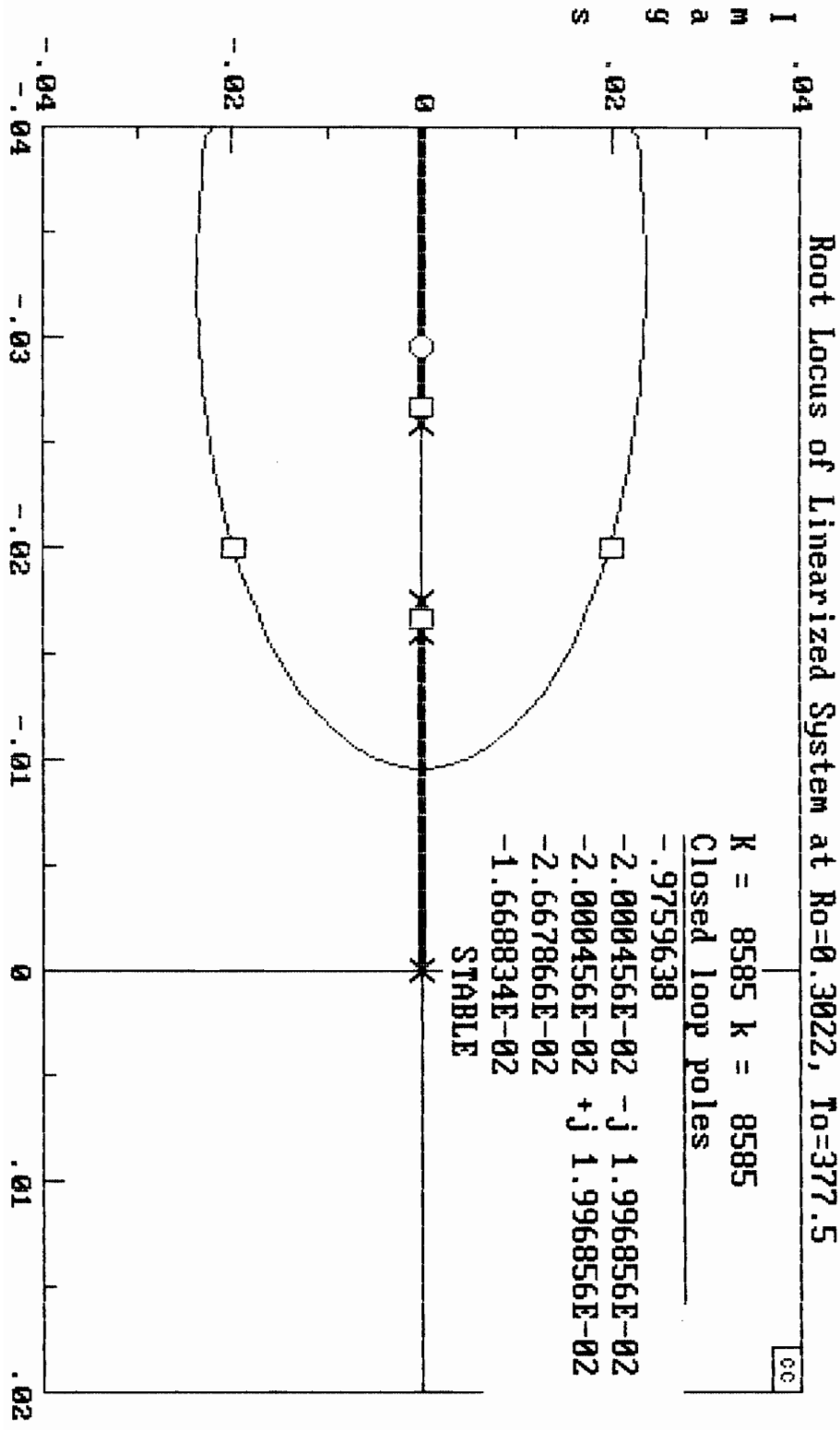
Root Locus of Linearized System at Ro=0.3022, To=377.5
K = 8585 k = 8585
Closed loop poles
-.9759638
-2.000456E-02 -j 1.996856E-02
-2.000456E-02 +j 1.996856E-02
-2.667866E-02
-1.668834E-02
STABLE
Imag
s
.04
.02
0
-.02
-.04
-.04
-.03
-.02
-.01
0
.01
.02

Figure 8

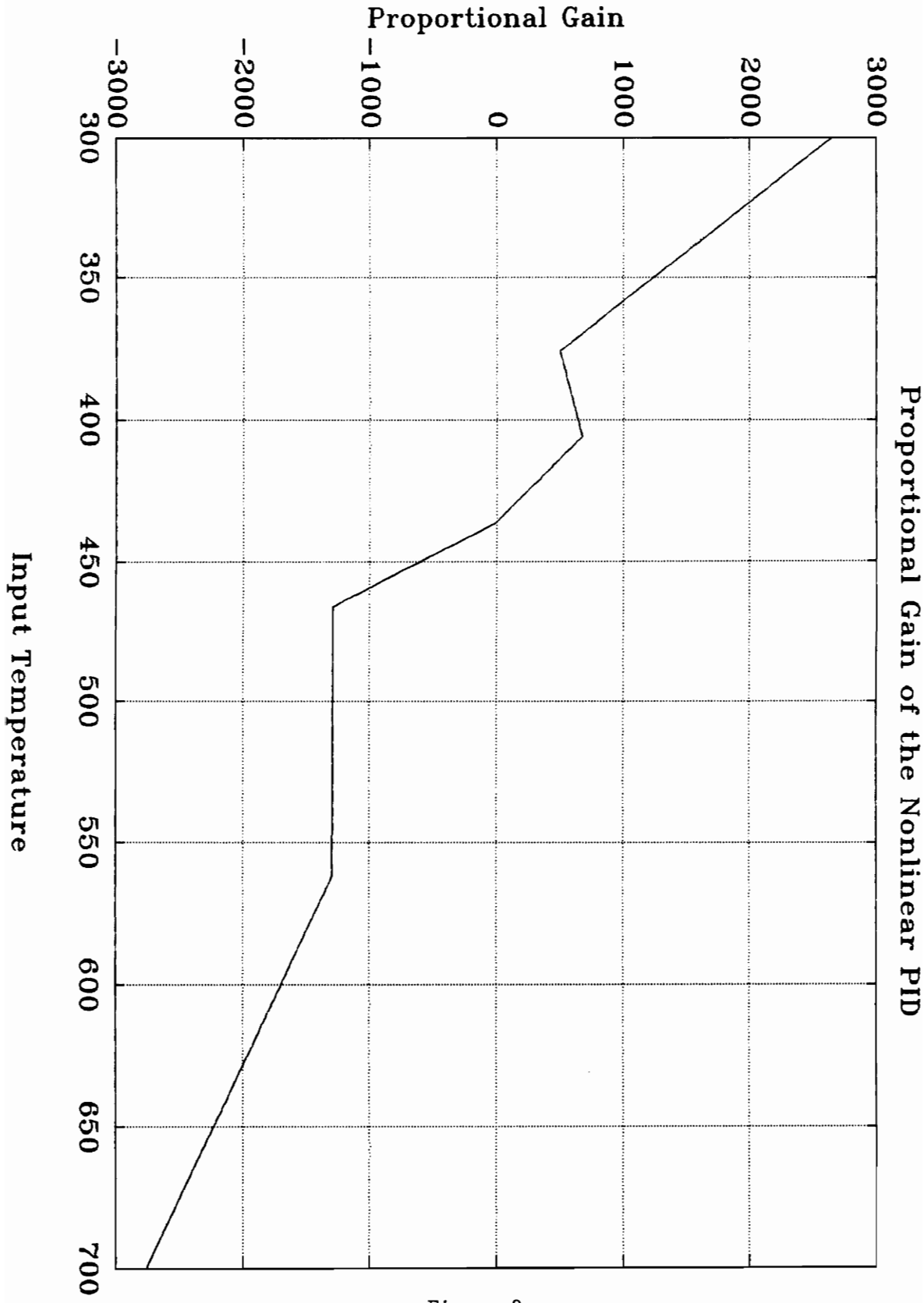
Proportional Gain of the Nonlinear PID
Proportional Gain
3000
2000
1000
0
−1000
−2000
−3000
300
350
400
450
500
550
600
650
700
Input Temperature

Figure 9

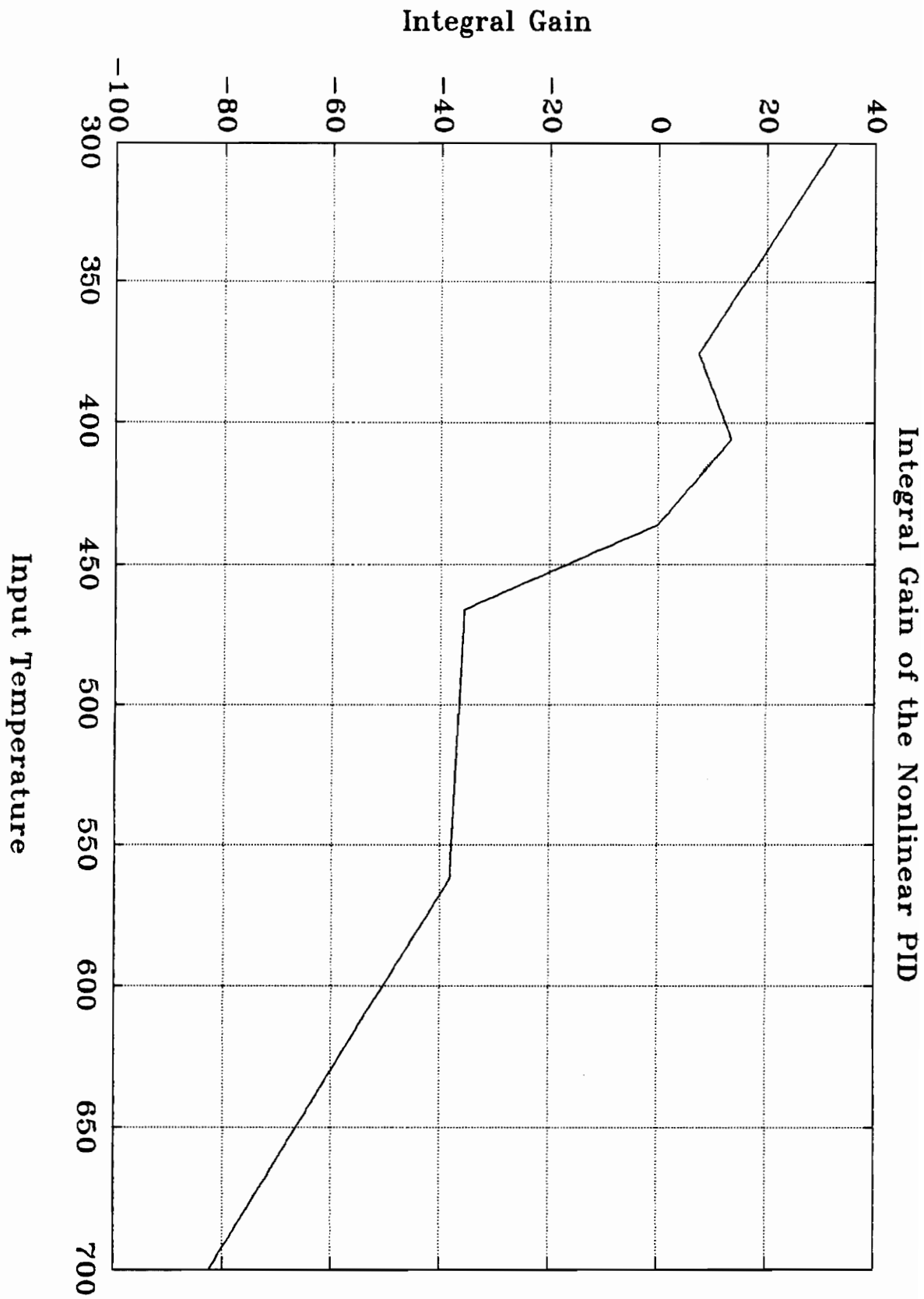
Integral Gain of the Nonlinear PID
Integral Gain
40
20
0
-20
-40
-60
-80
-100
300
350
400
450
500
550
600
650
700
Input Temperature

Figure 10

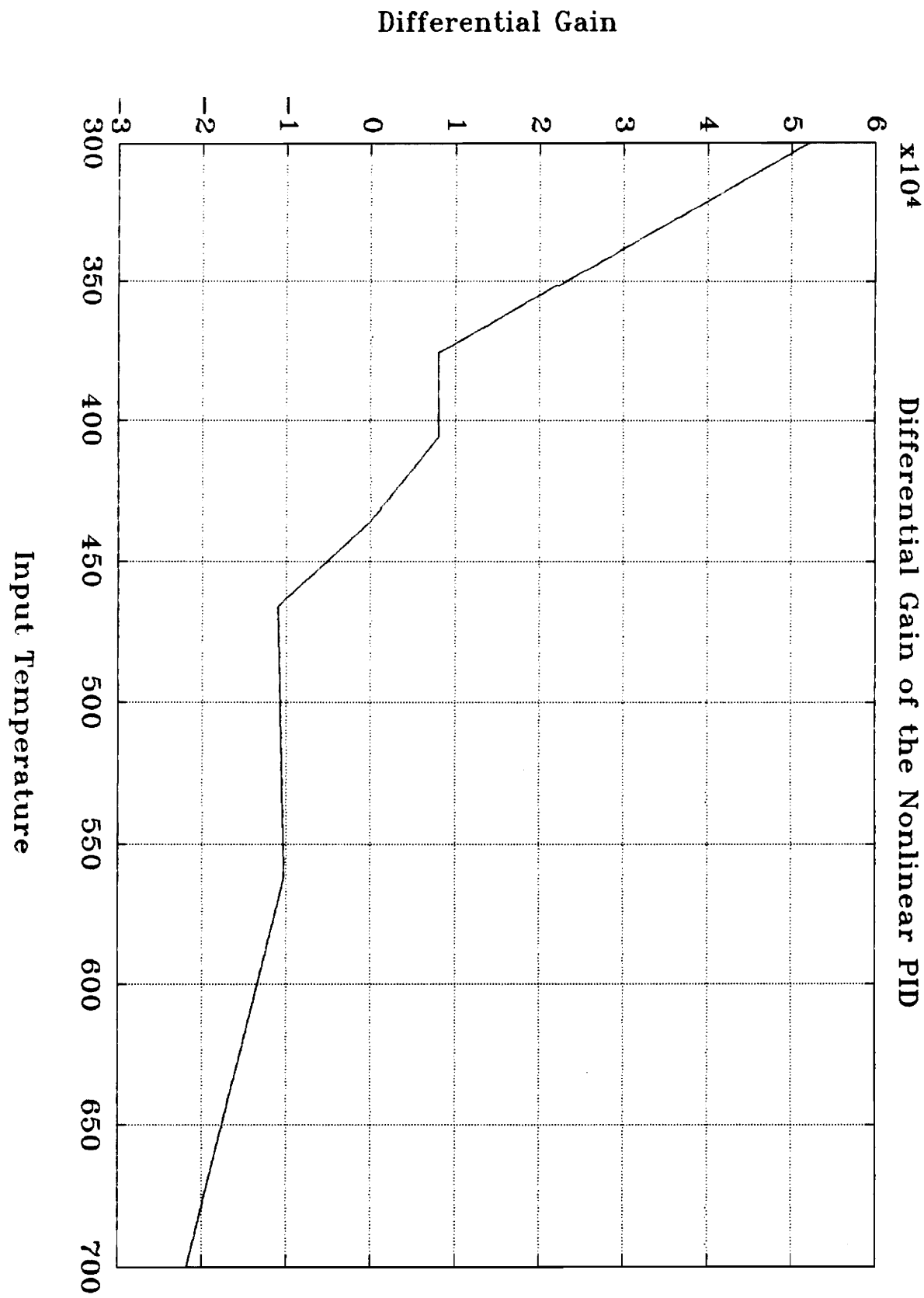
Differential Gain
Differential Gain of the Nonlinear PID
x10⁴
6
5
4
3
2
1
0
-1
-2
-3
300
350
400
450
500
550
600
650
700
Input Temperature

Figure 11

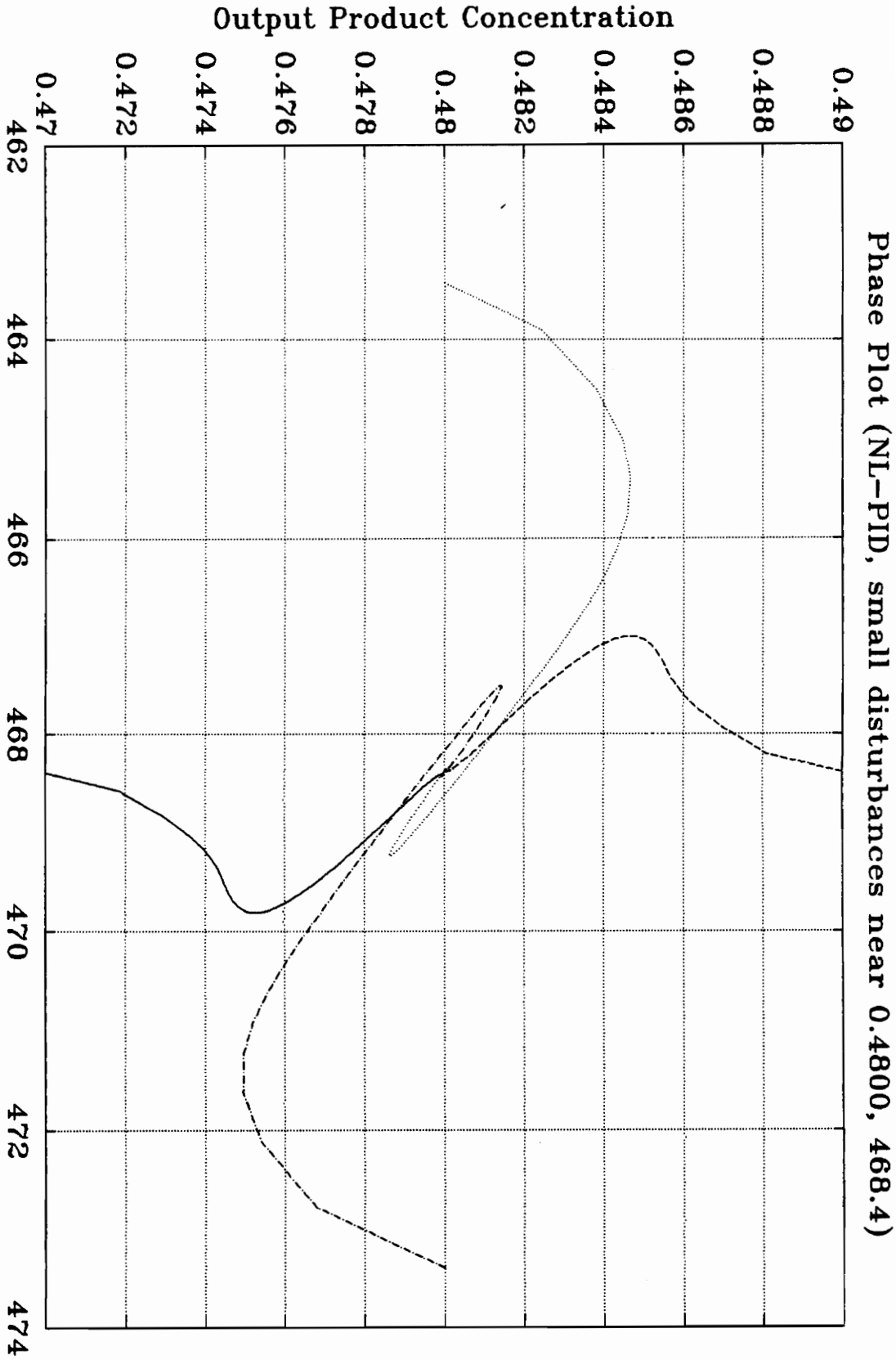
Phase Plot (NL-PID, small disturbances near 0.4800, 468.4)
Output Product Concentration
0.49
0.488
0.486
0.484
0.482
0.48
0.478
0.476
0.474
0.472
0.47
462
464
466
468
470
472
474
Output Temperature

Figure 12

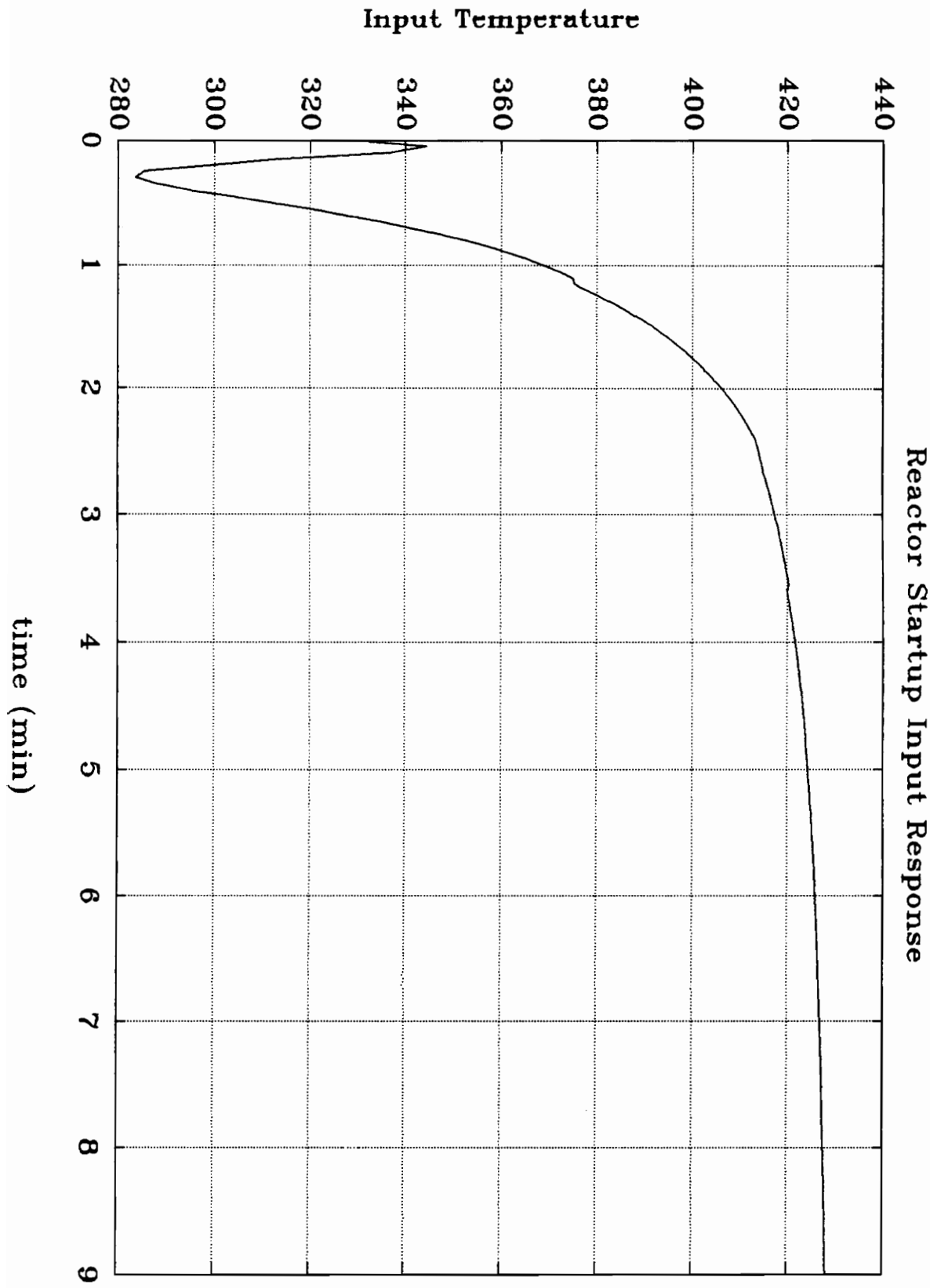
Reactor Startup Input Response
Input Temperature
440
420
400
380
360
340
320
300
280
0
1
2
3
4
5
6
7
8
9
time (min)

Figure 13

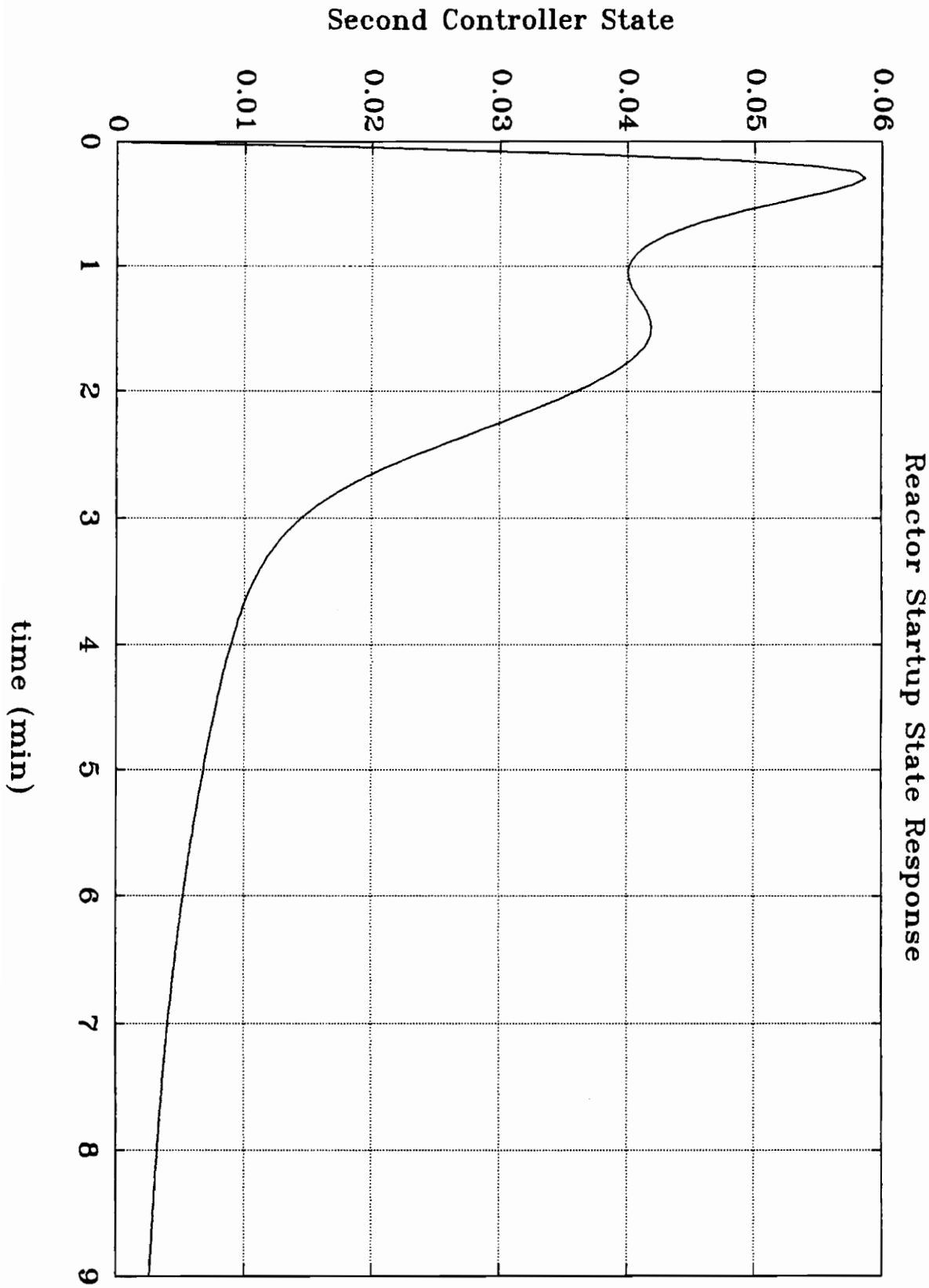
Reactor Startup State Response
Second Controller State
0.06
0.05
0.04
0.03
0.02
0.01
0
0
1
2
3
4
5
6
7
8
9
time (min)

Figure 14

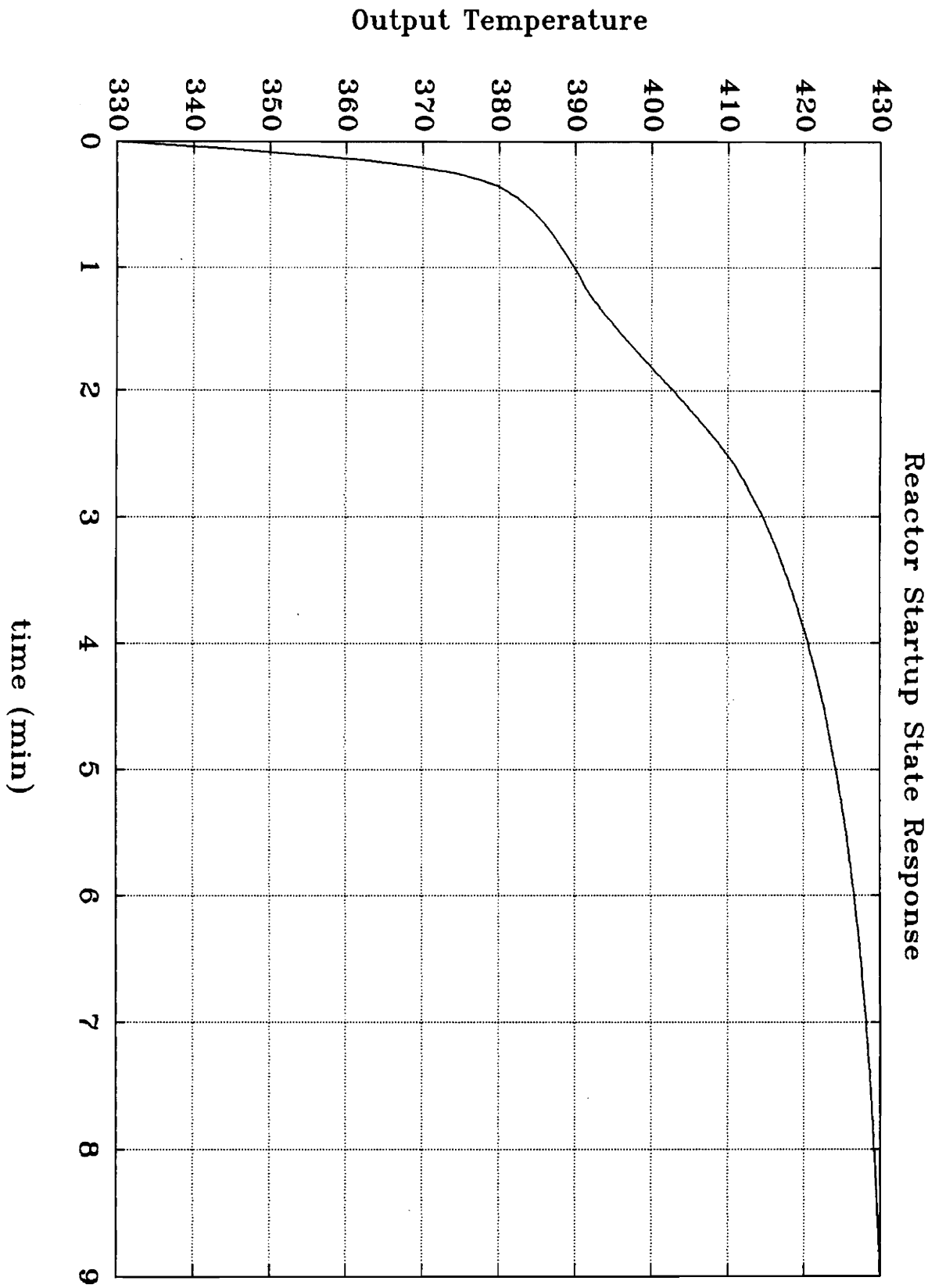
Reactor Startup State Response
Output Temperature
430
420
410
400
390
380
370
360
350
340
330
0
1
2
3
4
5
6
7
8
9
time (min)

Figure 15

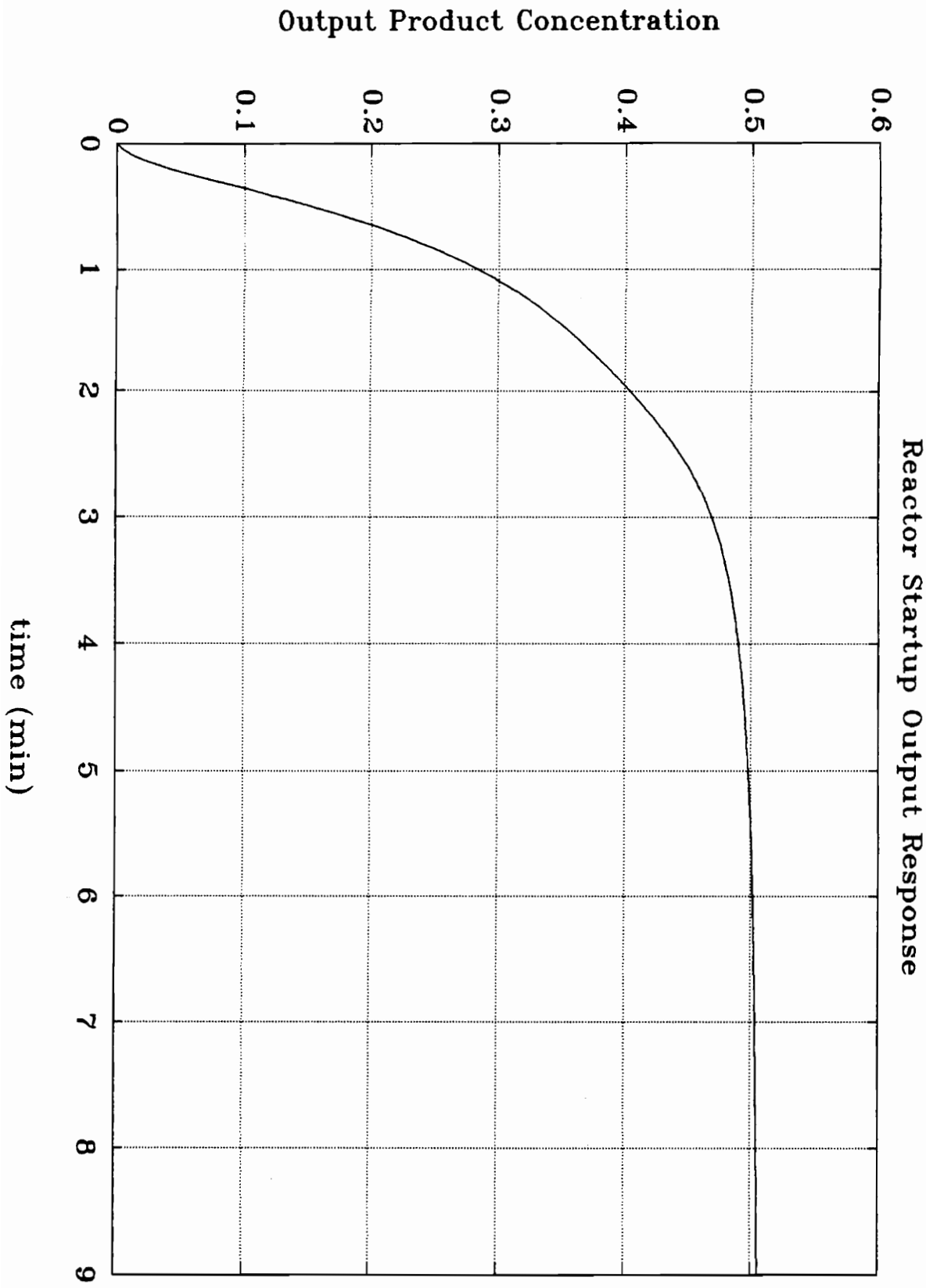
Reactor Startup Output Response
Output Product Concentration
0.6
0.5
0.4
0.3
0.2
0.1
0
0
1
2
3
4
5
6
7
8
9
time (min)

Figure 16

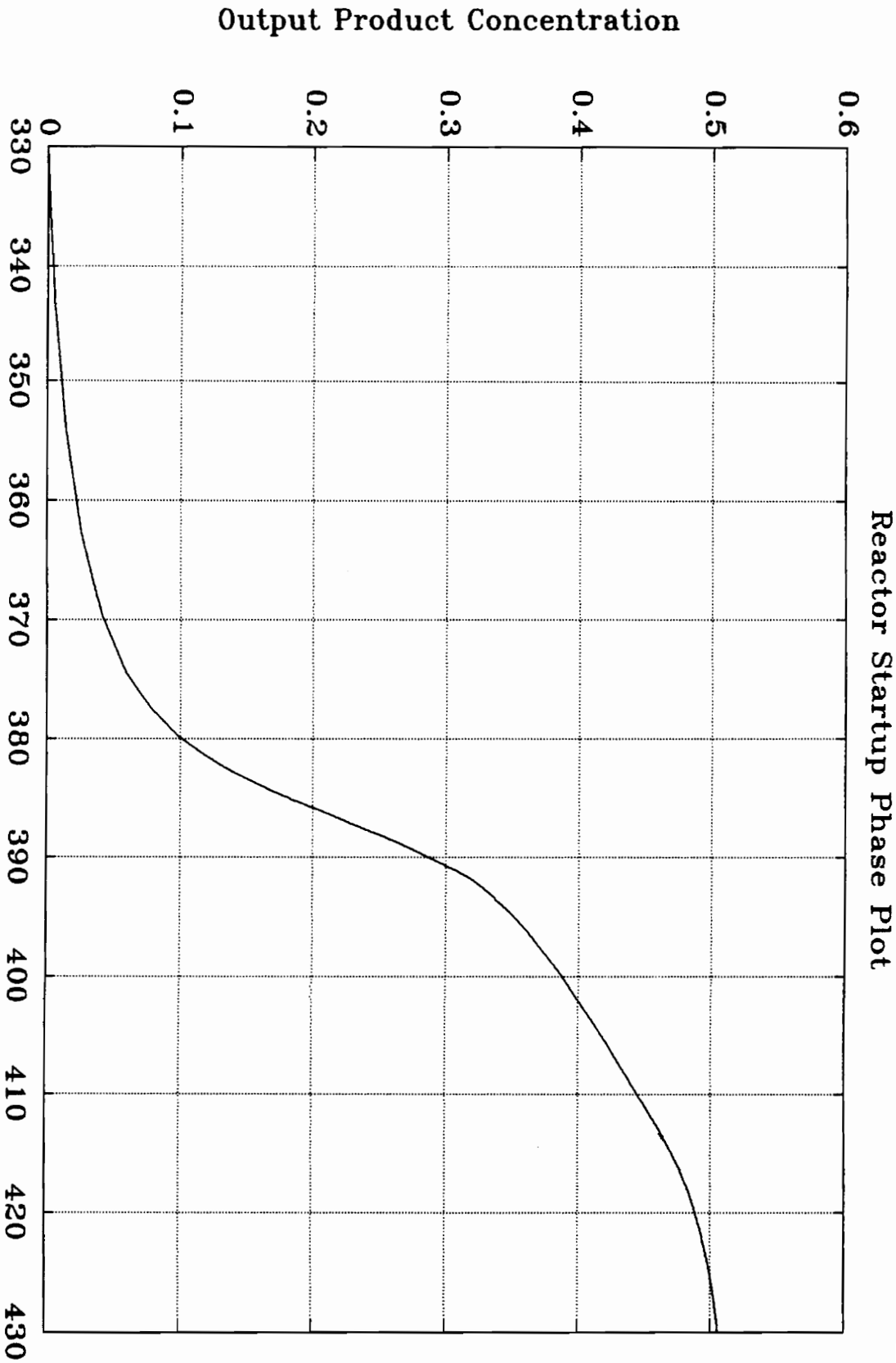
Reactor Startup Phase Plot
Output Product Concentration
0.6
0.5
0.4
0.3
0.2
0.1
0
330
340
350
360
370
380
390
400
410
420
430
Output Temperature

Figure 17

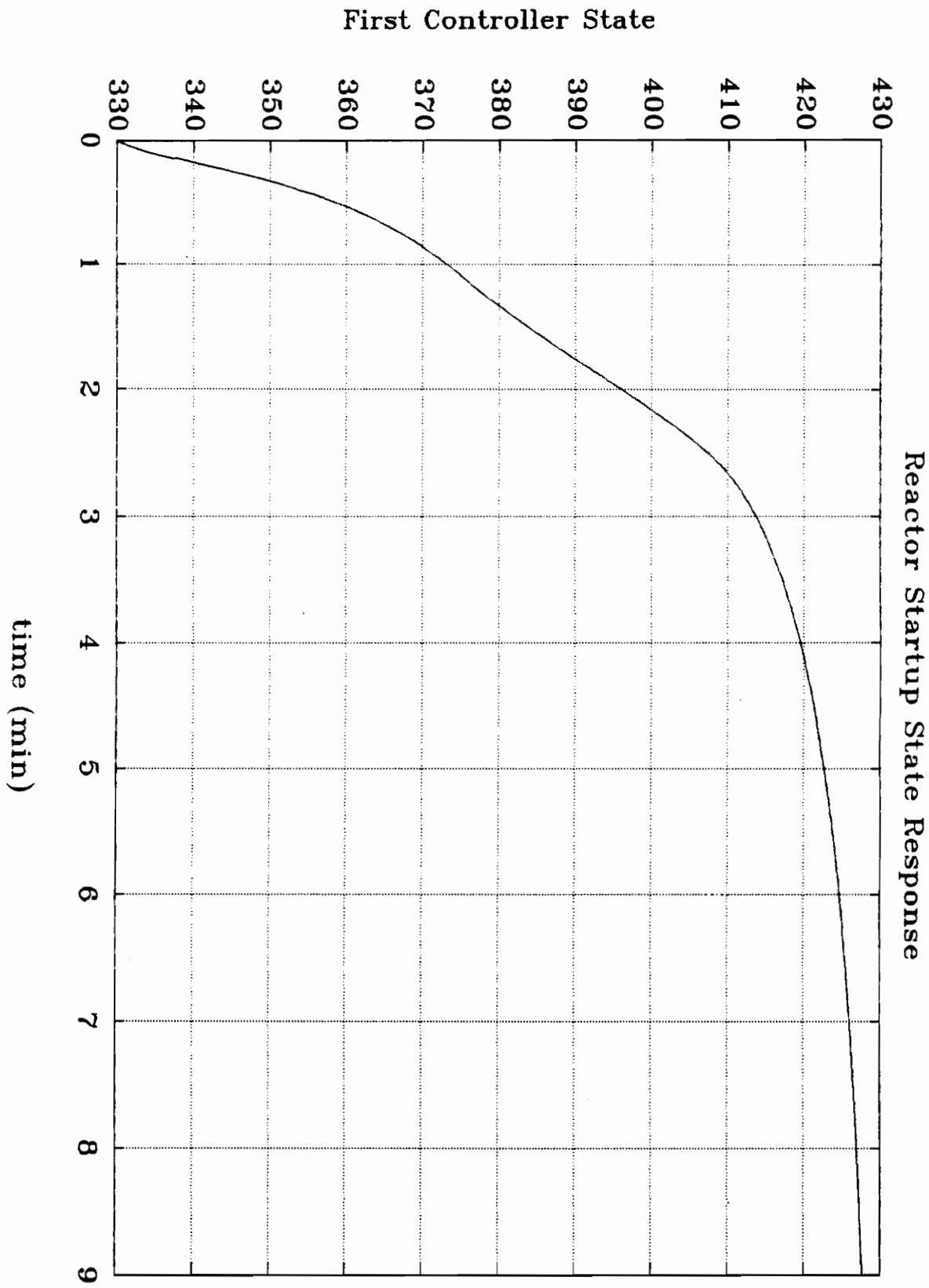
Reactor Startup State Response
First Controller State
430
420
410
400
390
380
370
360
350
340
330
0
1
2
3
4
5
6
7
8
9
time (min)

Figure 18

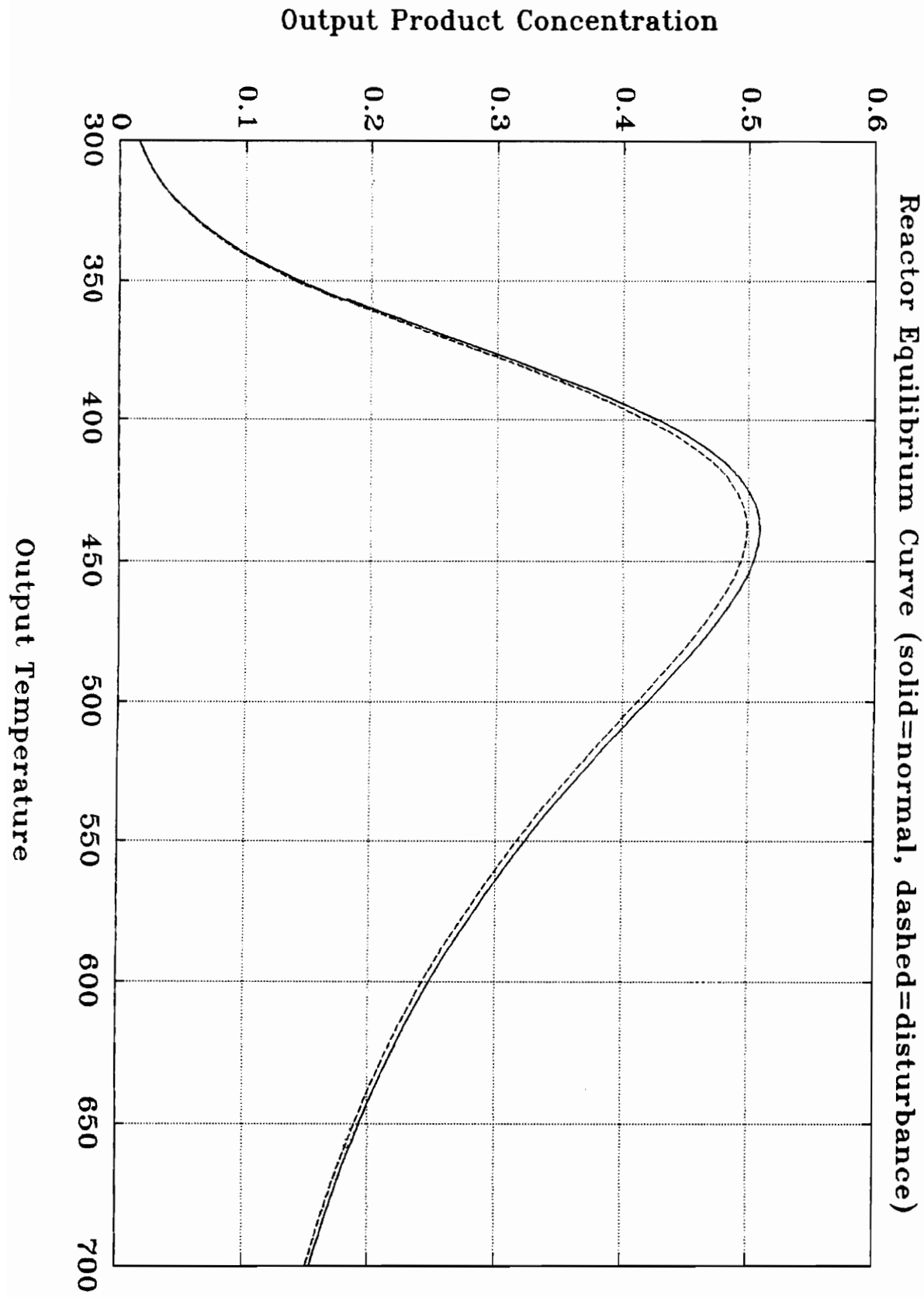
Reactor Equilibrium Curve (solid=normal, dashed=disturbance)
Output Product Concentration
0.6
0.5
0.4
0.3
0.2
0.1
0
300
350
400
450
500
550
600
650
700
Output Temperature

Figure 19

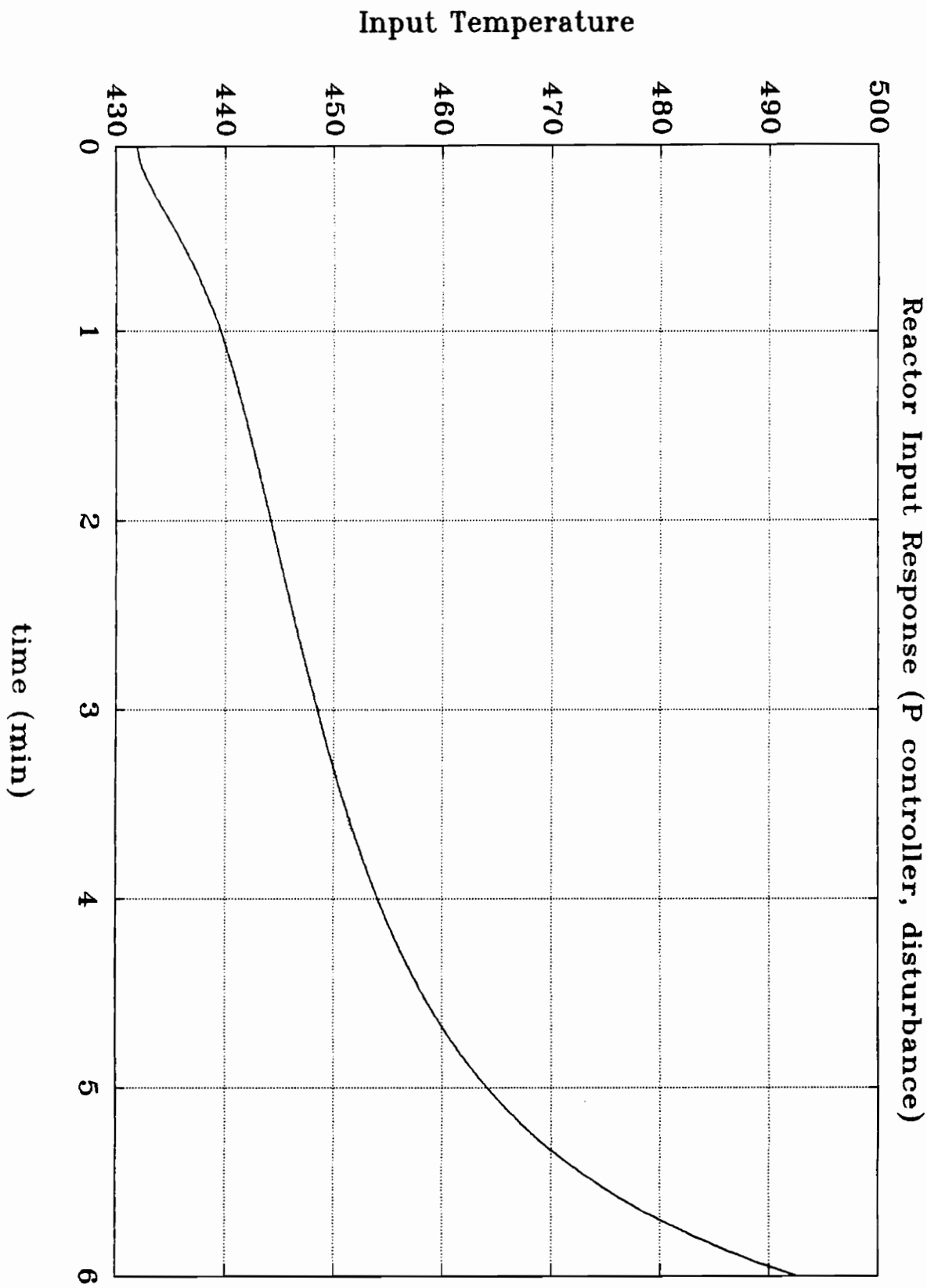
Reactor Input Response (P controller, disturbance)
Input Temperature
500
490
480
470
460
450
440
430
0
1
2
3
4
5
6
time (min)

Figure 20

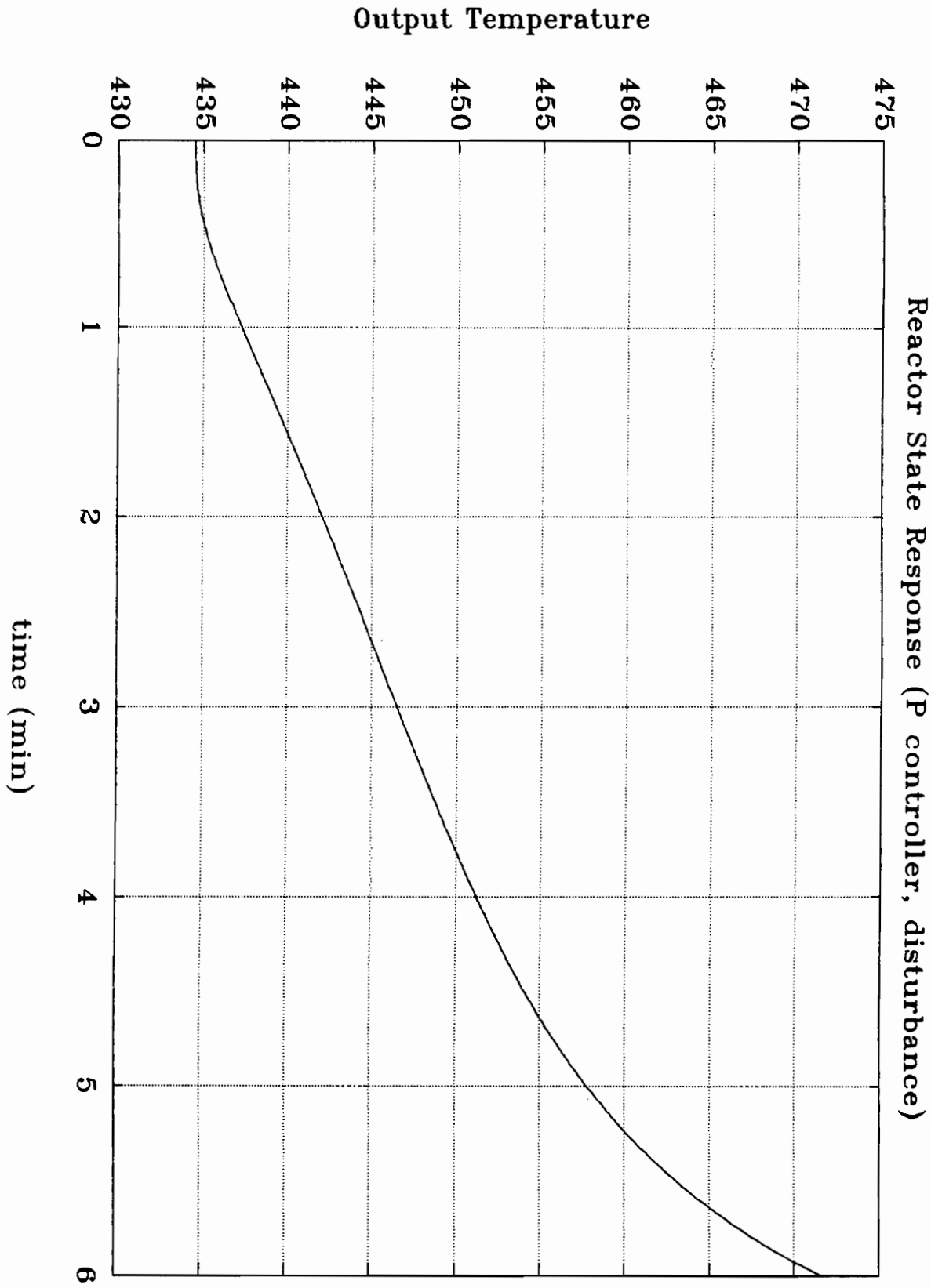
Reactor State Response (P controller, disturbance)
Output Temperature
475
470
465
460
455
450
445
440
435
430
0
1
2
3
4
5
6
time (min)

Figure 21

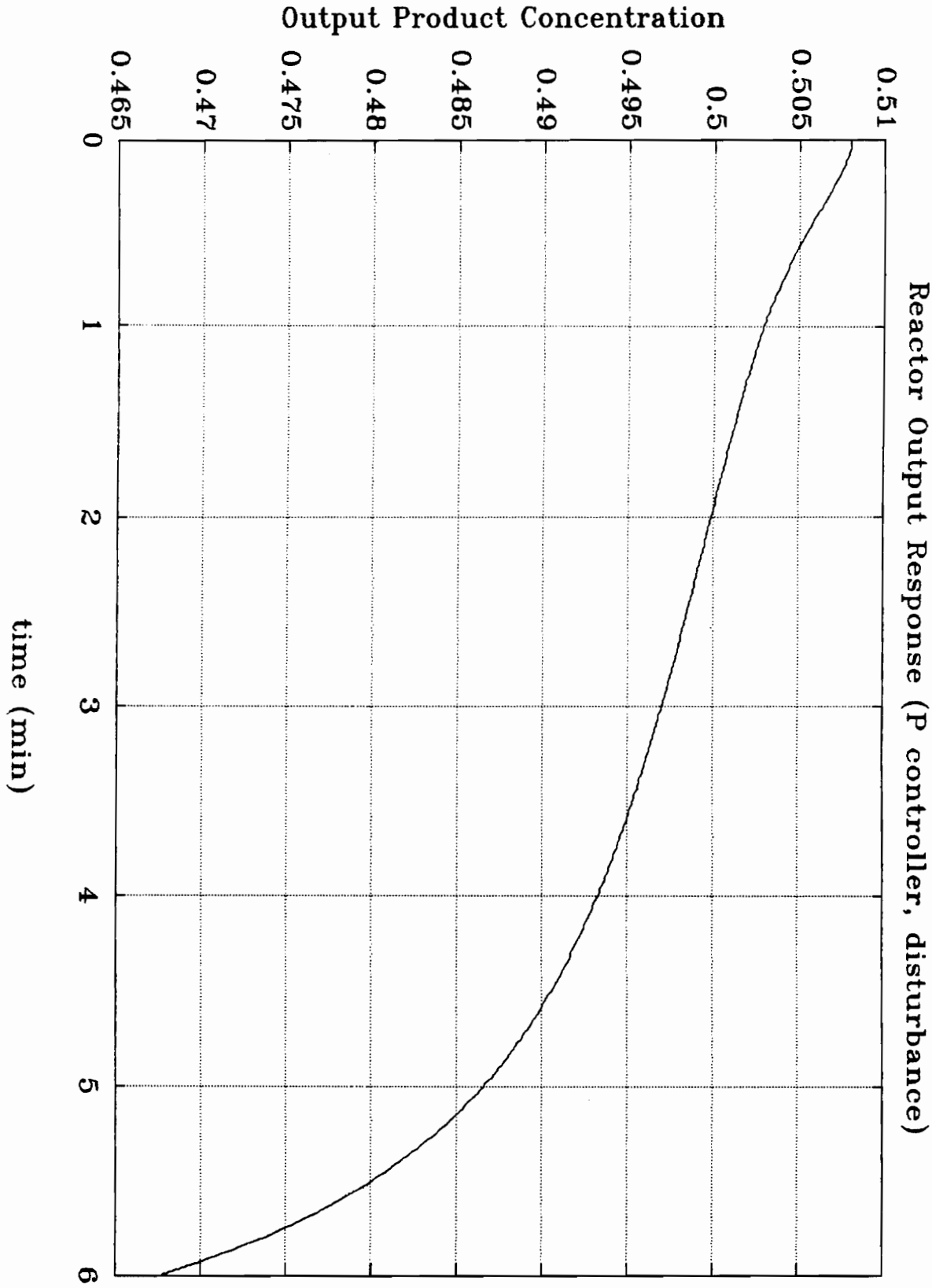
Reactor Output Response (P controller, disturbance)
Output Product Concentration
0.51
0.505
0.5
0.495
0.49
0.485
0.48
0.475
0.47
0.465
0
1
2
3
4
5
6
time (min)

Figure 22

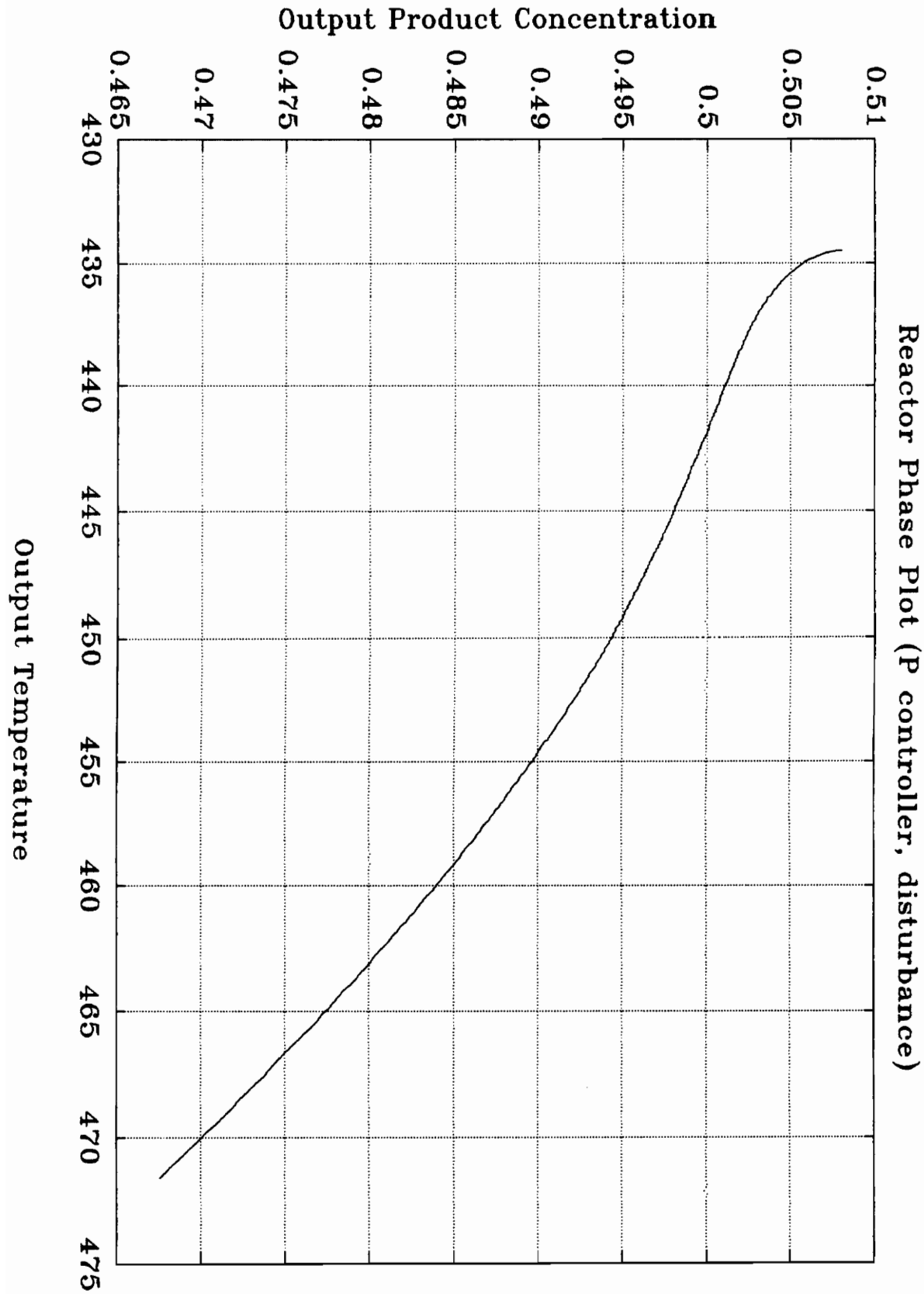
Reactor Phase Plot (P controller, disturbance)
Output Product Concentration
0.51
0.505
0.5
0.495
0.49
0.485
0.48
0.475
0.47
0.465
430
435
440
445
450
455
460
465
470
475
Output Temperature

Figure 23

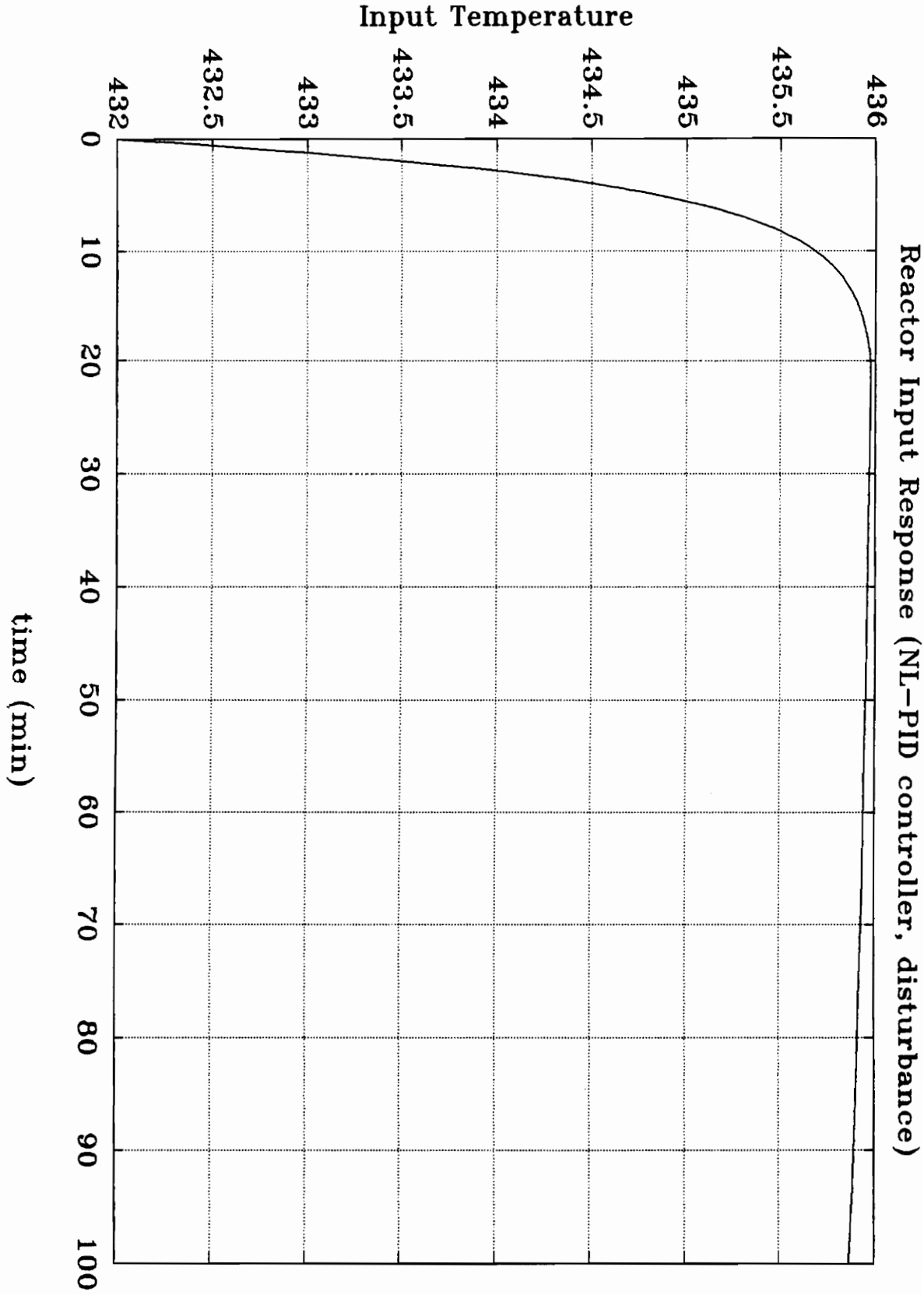
Reactor Input Response (NL-PID controller, disturbance)
Input Temperature
436
435.5
435
434.5
434
433.5
433
432.5
432
0
10
20
30
40
50
60
70
80
90
100
time (min)

Figure 24

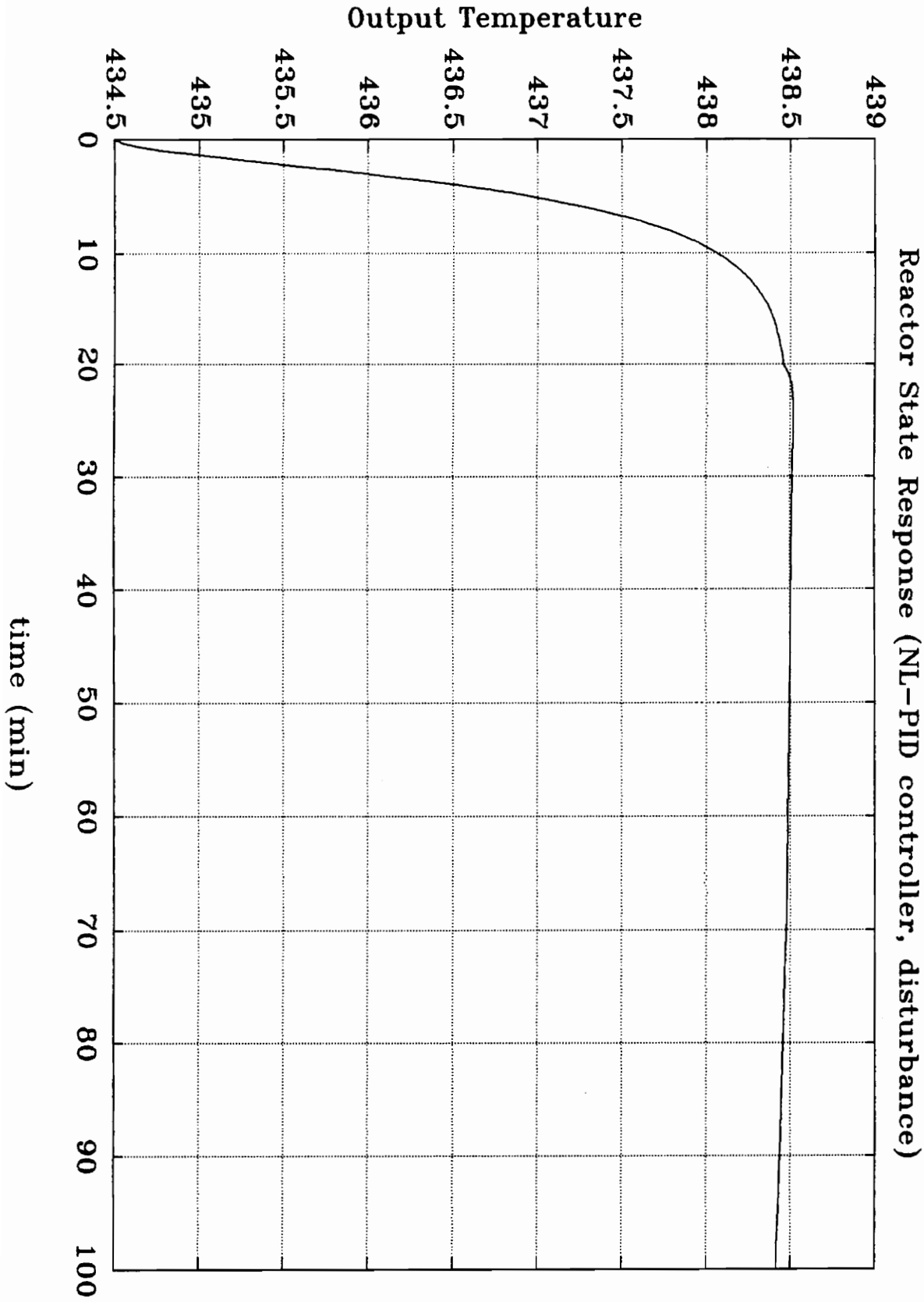
Reactor State Response (NL-PID controller, disturbance)
Output Temperature
439
438.5
438
437.5
437
436.5
436
435.5
435
434.5
0
10
20
30
40
50
60
70
80
90
100
time (min)

Figure 25

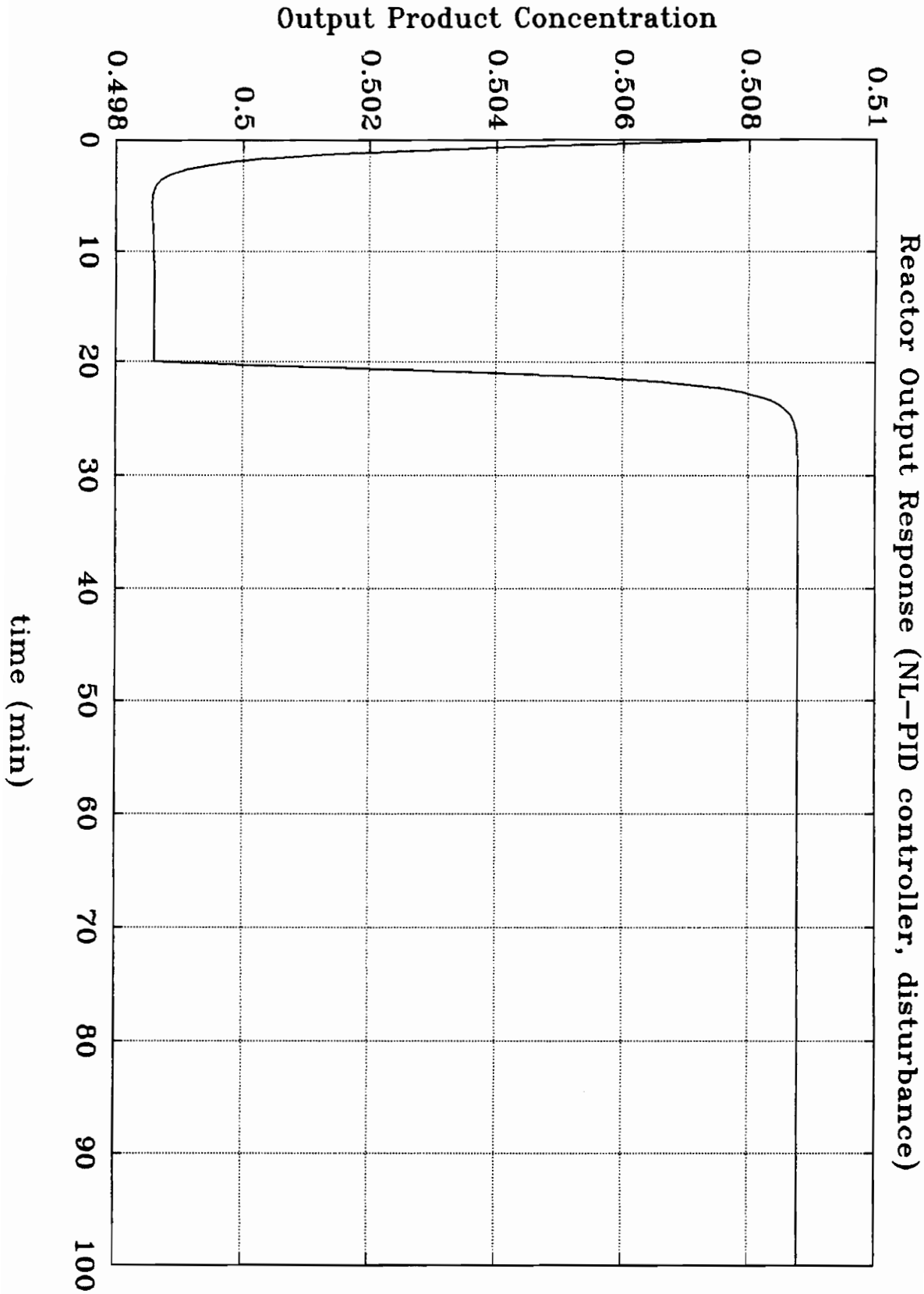
Reactor Output Response (NL-PID controller, disturbance)
Output Product Concentration
0.51
0.508
0.506
0.504
0.502
0.5
0.498
0
10
20
30
40
50
60
70
80
90
100
time (min)

Figure 26

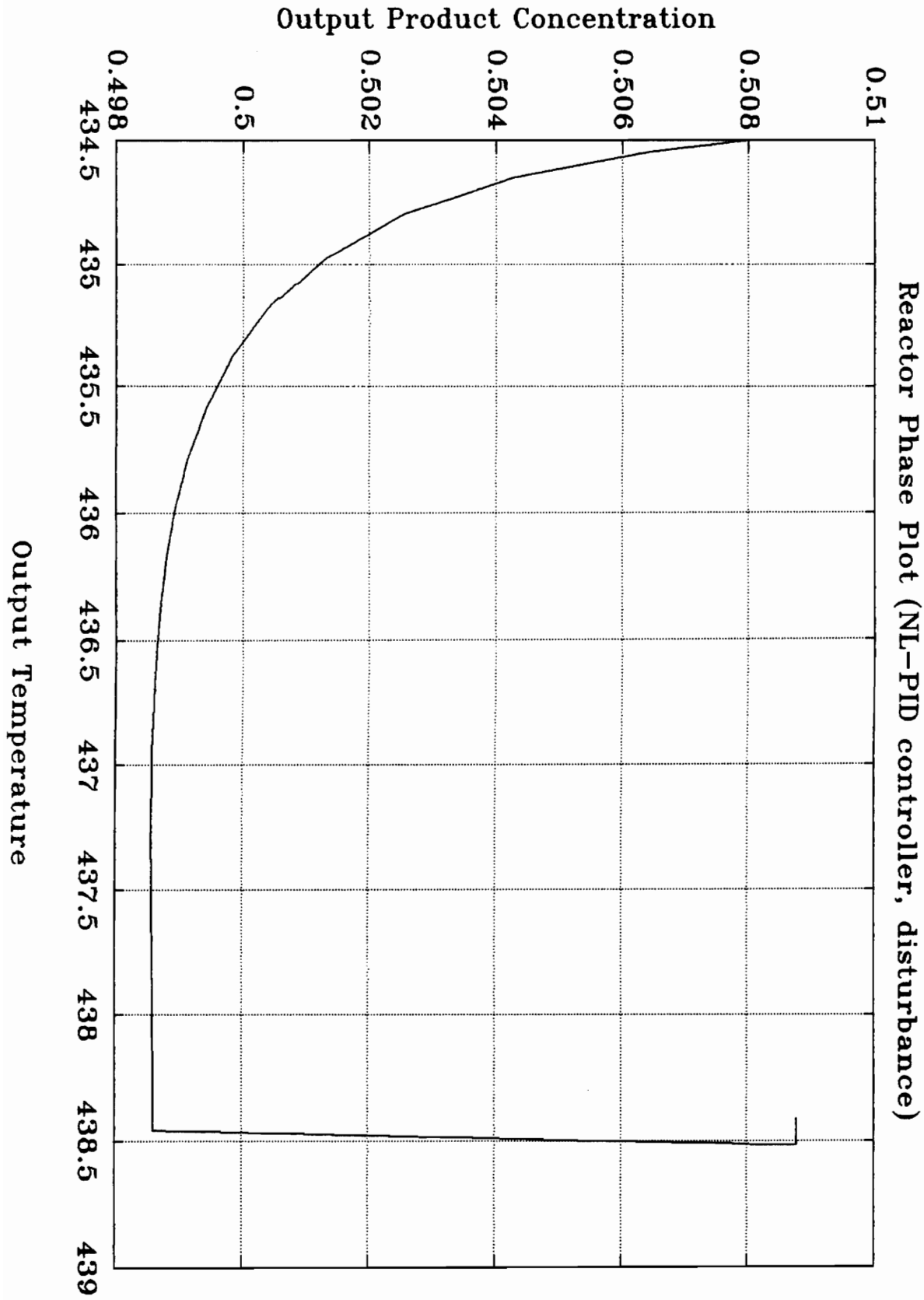
Reactor Phase Plot (NL-PID controller, disturbance)
Output Product Concentration
0.51
0.508
0.506
0.504
0.502
0.5
0.498
434.5
435
435.5
436
436.5
437
437.5
438
438.5
439
Output Temperature

Figure 27

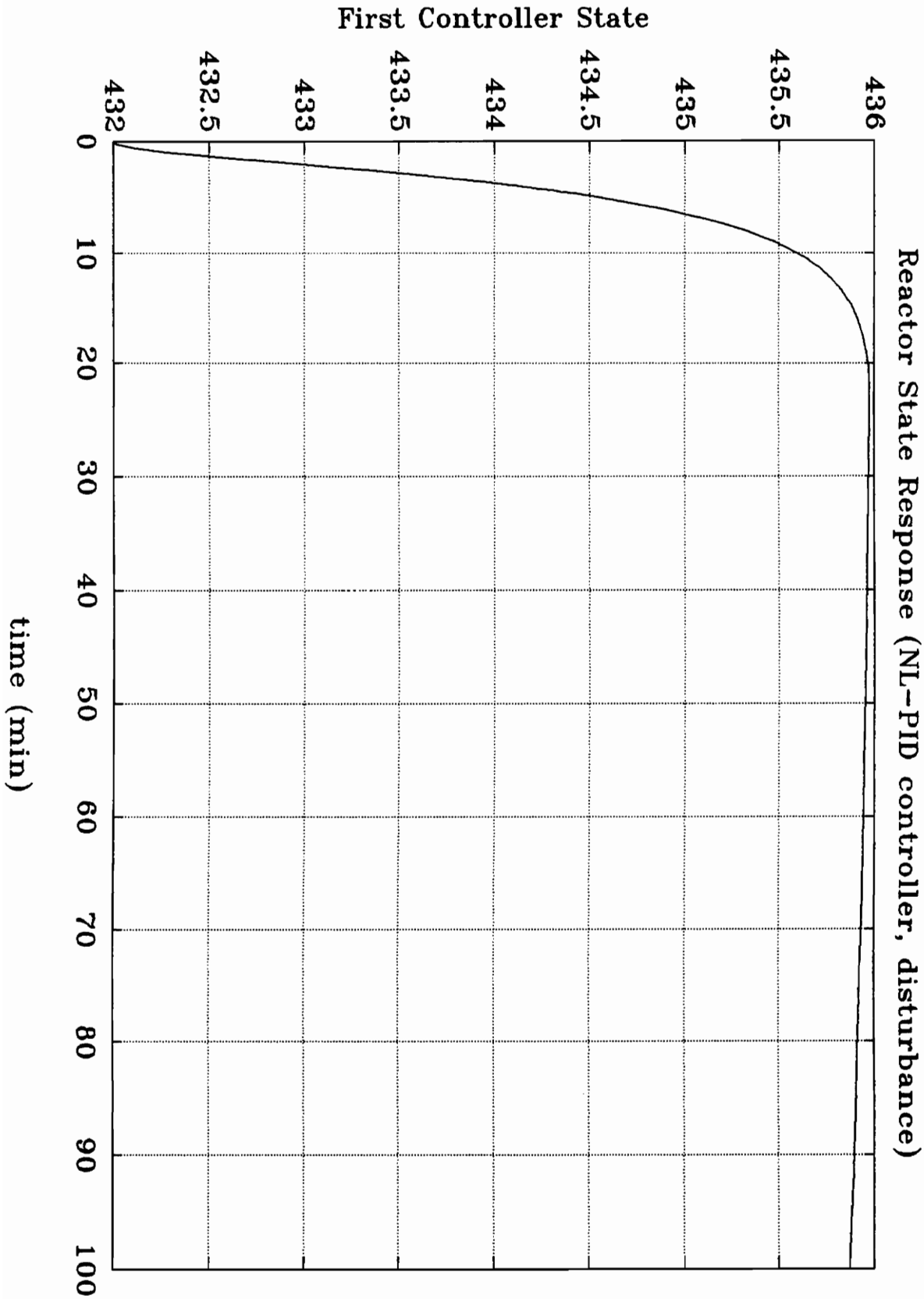
Reactor State Response (NL-PID controller, disturbance)
First Controller State
436
435.5
435
434.5
434
433.5
433
432.5
432
0
10
20
30
40
50
60
70
80
90
100
time (min)

Figure 28

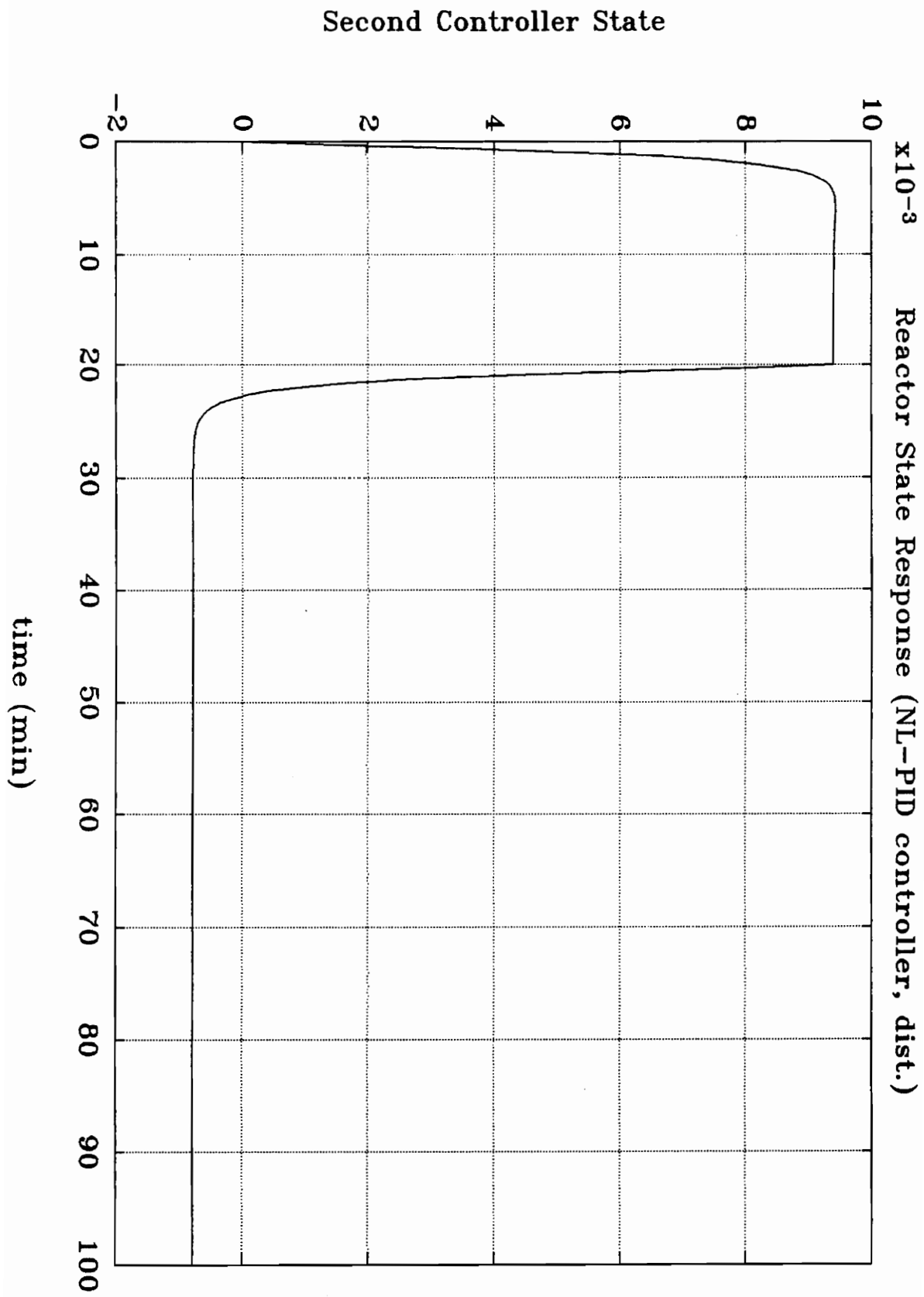
Second Controller State
x10-3
Reactor State Response (NL-PID controller, dist.)
10
8
6
4
2
0
-2
0
10
20
30
40
50
60
70
80
90
100
time (min)

Figure 29

CHAPTER 5

Towards A Unified Framework ?

When an industrial system has dynamics that change substantially over the operating range of interest (especially true of nonlinear systems), adaptive control schemes are a viable alternative to fixed parameter control schemes. The self-adaptive control scheme referred to as 'gain scheduling', where the controller parameters are scheduled as functions of a plant variable, is in wide use and is the basis for the nonlinear PID design scheme in this thesis. The purpose of this chapter is to examine other nonlinear PID design schemes and to determine if the one presented in this thesis provides a unified framework.

In Marini and Georgakis(1984), a two part study of low-density vessel reactors is undertaken. Part 1 presents a three stage model for the reactor and Part 2 shows that a linear controller cannot operate the system over the entire range of interest, thereby suggesting some form of adaptive control. The unstable dynamics of the reactor are shown to be related to the deviation of the reaction rate $R(M(t),T(t),I_o(t))$ from its equilibrium value $R(M_s,T_s,I_{os})$, where M is the monomer concentration, T is the polymerization temperature, I_o is the initiator feed and the s subscript indicates an equilibrium value. This suggests that the controller be based on this reaction rate deviation and an ideal nonlinear controller expression which controls I_o to keep the reaction rate at its steady-state value is obtained:

$$R(M(t),T(t),I_o(t)) = R(M_s,T_s,I_{os}) \tag{5.1}$$

The closed-loop dynamics of the system with this controller are:

$$\dot{x}_1 = -x_1 \tag{5.2}$$

$$\dot{x}_2 = -x_2 \tag{5.3}$$

where $x_1 = M - M_s$ and $x_2 = T - T_s$. These equations are obtained without linearization and are valid for any magnitude of x_1 and x_2. Therefore, the reactor is always closed-loop stable. An ideal linearized controller expression is calculated as:

$$U = -\left[\frac{R_1}{R_3}\cdot x_1 + \frac{R_2}{R_3}\cdot x_2\right] \tag{5.4}$$

where $U = I_o - I_{os}$ and R_1, R_2, and R_3 are described as:

$$R_1 = \frac{\partial R}{\partial M}\bigg|_{M_s,T_s,I_{os}} \tag{5.5}$$

$$R_2 = \frac{\partial R}{\partial T}\bigg|_{M_s,T_s,I_{os}} \tag{5.6}$$

$$R_3 = \frac{\partial R}{\partial I_o}\bigg|_{M_s,T_s,I_{os}} \tag{5.7}$$

At this point the following assumptions are made: the total enthalpy, $\beta\cdot M + T$ (where β is the dimensionless heat of reaction), of the reactor is always at steady state; the monomer concentration in all three stages of the reactor is the same; the contribution of the first two stages of the reactor to the reaction rate R is negligible; and in each stage, the radicals termination rate is equal to the production rate. This leads to the final form of the

controller:

$$U = I_s \cdot \left[\frac{F^2(T_s)}{F^2(T)} + K_c' \cdot (T_s - T) + \frac{K_c'}{\tau_i'} \cdot \left[\int (T_s - T) \cdot dt \right] \right] \tag{5.8}$$

$$F(T) = Da \cdot \exp\left[\gamma \cdot \left[1 - \frac{1}{T} \right] \right] \cdot \sqrt{\frac{r_i}{(1 + r_i + \alpha \cdot r_i^2)}} \tag{5.9}$$

$$r_i = Da_I \cdot \exp\left[\gamma_I - \frac{\gamma_I}{T} \right] \tag{5.10}$$

where I_s is the steady state value of initiator concentration, K_c' and τ_i' are similar to tuning parameters used in classical PI controllers, γ_I is the dimensionless initiator activation energy, α takes into account the fluid dynamic characteristics of the reactor model, r_i is the initiator decomposition rate, and Da_I is the initiator Damkohler number. This is a linear PI controller with an additional term that takes into account the nonlinearities of the reactor model. The chosen operating equilibrium values of initiator concentration I_s and reactor temperature T_s will determine the controller gains and the magnitude of the nonlinear term. The $(T_s - T)$ term in the controller equation is the error term. This nonlinear 'reaction rate' controller does not have the same general form as the nonlinear PID controller. The nonlinearity occurs in the controller equation independent of the proportional and integral gains, which are linear in nature. If the controller is linearized about a temperature equilibrium point, the resulting controller has gains that are function of a chosen operating point. The nonlinear PID gains are scheduled with respect to the input of the plant. Also, the purpose of this controller is not to extend the range of equilibrium point operation but

rather to stabilize the system about a single equilibrium point.

The nonlinear PID design scheme used by Jutan(1989) was suggested by Clark(1984), who wanted a controller with derivative action that didn't amplify excessive process measurement noise. Clark's suggestion was a PI controller with proportional gain variations based on the magnitude of the error such that with small errors the controller gain would be small, resulting in low noise amplification, but with large errors the larger controller gain would cause the system to have a faster response. The proportional gain is described by the equation:

$$K_p = K_0 \cdot \left[1 + K_1 \cdot |e(t)|\right] \tag{5.11}$$

Jutan's objections to Clark's controller are:

> ...the loss of derivative information would be a serious impediment for controlling processes with large time constants. Also, we believe that information on the trend of past errors, in addition to the magnitude of the current error, is important in determining the current control action.

Jutan modifies the variable proportional gain in Clark's controller such that a trend function as well as the magnitude of the error determines the proportional gain. The controller is given by:

$$m(t) = K_c \cdot \left[\left[e(t) - \alpha \cdot \beta(t) \cdot |e(t)|\right] + \frac{1}{T_i} \cdot \left[\int e(t) \cdot dt\right]\right] \tag{5.12}$$

where m(t) is the controller output, K_c is the proportional constant, e(t) is the process error, α is a tuning constant for the nonlinear term, $\beta(t)$ is the trend function, and T_i is the integral constant. The trend function $\beta(t)$ is a linear regression estimate based on current and previous process measurements and is described by:

$$\beta(t) = \frac{0.3\cdot\left[y(t) - y(t - 3\cdot T)\right] + 0.1\cdot\left[y(t - T) - y(t - 2\cdot T)\right]}{T} \tag{5.13}$$

This is preferred over a trend function based on the error since set point changes would cause rapid error trend fluctuations. The resulting trend function has less trend change response than a differentiator, but has less noise sensitivity. Jutan goes on to develop ITAE tuning formulae for this controller and to show through simulations that this controller has better performance and less noise sensitivity than a linear PID. This nonlinear PI(D) controller is basically a PI controller with the proportional gain scheduled as a function of the output of the plant and thus has same general form as the nonlinear PID controller in this thesis. The purpose of this controller is to provide better performance with respect to a single equilibrium point, not a range of equilibrium points.

In Alvarez, Alvarez and Gonzalez(1989), a global nonlinear control law is developed for a nonlinear continuous stirred tank reactor (CSTR). The CSTR is modeled by:

$$\dot{c} = \frac{\omega}{V}\cdot(c_e - c) - k_o\cdot c\cdot e^{\left[\frac{-E_a}{R\cdot T}\right]} \tag{5.14}$$

$$\dot{T} = \frac{\omega}{V}\cdot(T_e - T) - \frac{h_w\cdot A_w}{V\cdot\rho\cdot c_p}\cdot(T - T_c) + \frac{(-\Delta H)}{\rho\cdot c_p}\cdot k_o\cdot c\cdot e^{\left[\frac{-E_a}{R\cdot T}\right]} \tag{5.15}$$

where c is the reactor concentration, ω is the volumetric flow rate, V is the reactor volume, c_e is the feed concentration, k_o is the frequency factor for first-order kinetics, E_a is the activation energy, R is the universal gas constant, T is the reactor temperature, T_e is the feed temperature, h_w is the heat transfer coefficient, A_w is the heat transfer area, ρ is the fluid density, c_p is the fluid specific heat capacity, T_c is the coolant temperature and $(-\Delta H)$ is the reaction heat generation per mole reacted. If an equilibrium point is chosen as an operating point and the equilibrium values of the state and input values are represented by by $\bar{c}$, $\overline{T}$, $\bar{c}_e$, $\overline{T}_e$ and $\overline{T}_c$ then the reactor model can be rewritten as:

$$\dot{x} = f(x) + g\cdot u: \ x,f,g \in R^2 \text{ and } u \in R \tag{5.16}$$

$$f_1(x_1,x_2) = \theta\cdot\bar{c}_e - \theta\cdot(\bar{c} + x_1) - \alpha\cdot(\bar{c} + x_1)\cdot e^{\left[\frac{-\delta}{(\overline{T} + x_2)}\right]} \tag{5.17}$$

$$f_2(x_1,x_2) = \theta\cdot\overline{T}_e + \gamma\cdot\overline{T}_c - (\theta + \gamma)\cdot(\overline{T} + x_2) + \alpha\cdot\beta\cdot(\bar{c} + x_1)\cdot e^{\left[\frac{-\delta}{(\overline{T} + x_2)}\right]} \tag{5.18}$$

$$g_1 = 0,\ g_2 = \gamma \tag{5.19-5.20}$$

where $x_1 = c - \bar{c}$, $x_2 = T - \overline{T}$, $u = T_c - \overline{T}_c$ are deviation variables and the new parameters are defined as $\alpha = k_o$, $\theta = \frac{\omega}{V}$, $\delta = \frac{E_a}{R}$, $\beta = \frac{(-\Delta H)}{(\rho\cdot c_p)}$, and $\gamma = \frac{h_w\cdot A_w}{(V\cdot\rho\cdot c_p)}$. The desired control law is described by:

$$u = p(x), \qquad p{:}W \rightarrow R \tag{5.21}$$

where W is an open, connected set in R^2 where the functioning of the controller is assured. Both p and W depend on the selection of a particular equilibrium point as the operating point. Differential-geometric techniques are used to transform the nonlinear system to a linear system. The authors point out that the definition of globality they use is not a property over the plane but is:

> ...to designate a property over a well-defined domain as contrasted to a neighborhood about a point.

This definition of globality is the basis for the development of nonlinear controllability, transformability, and asymptotic stability for a particular operating region in general. After designing linear P and PI controllers for the linear system, a transformation back to the original coordinates results in a global, nonlinear, two input P controller given by:

$$u = k_{p1} \cdot p_1(x_1,x_2) + k_{p2} \cdot p_2(x_1,x_2) + p_3(x_1,x_2) \tag{5.22}$$

$$p_1(x) = \frac{x_1}{\gamma \cdot f_{12}(x_1,x_2)} \tag{5.23}$$

$$p_2(x) = \frac{f_1(x_1,x_2)}{\gamma \cdot f_{12}(x_1,x_2)} \tag{5.24}$$

$$p_3(x) = -\frac{f_{11}(x_1,x_2) \cdot f_1(x_1,x_2)}{\gamma \cdot f_{12}(x_1,x_2)} - \frac{1}{\gamma} \cdot f_2(x_1,x_2) \tag{5.25}$$

and a global, nonlinear, two input PI controller given by:

$$u = k_{p1}\cdot p_1(x) + k_{p2}\cdot p_2(x) + k_{i1}\cdot p_3(x) + k_{i2}\cdot p_4(x) + p_5(x) \tag{5.26}$$

$$p_1(x) = \frac{x_1}{\gamma\cdot f_{12}(x_1,x_2)} \tag{5.27}$$

$$p_2(x) = \frac{f_1(x_1,x_2)}{\gamma\cdot f_{12}(x_1,x_2)} \tag{5.28}$$

$$p_3(x) = \frac{\int x_1\cdot dt}{\gamma\cdot f_{12}(x_1,x_2)} \tag{5.29}$$

$$p_4(x) = \frac{\int f_1(x_1,x_2)\cdot dt}{\gamma\cdot f_{12}(x_1,x_2)} \tag{5.30}$$

$$p_5(x) = -\frac{f_{11}(x_1,x_2)\cdot f_1(x_1,x_2)}{\gamma\cdot f_{12}(x_1,x_2)} - \frac{1}{\gamma}\cdot f_2(x_1,x_2) \tag{5.31}$$

where:

$$f_{11} = \frac{\partial f_1}{\partial x_1} = -\theta - \alpha\cdot e^{\left[\frac{-\delta}{(\bar{T} + x_2)}\right]} \tag{5.32}$$

$$f_{12} = \frac{\partial f_1}{\partial x_2} = -\frac{\alpha\cdot\delta\cdot(\bar{c} + x_1)\cdot e^{\left[\frac{-\delta}{(\bar{T} + x_2)}\right]}}{(\bar{T} + x_2)^2} \tag{5.33}$$

If the nonlinear PI controller is manipulated it can be made to resemble a two input, linear PID controller. If the nonlinear PI controller is rewritten as:

$$u = k^*_{p1}(x)\cdot x_1 + k^*_{p2}(x)\cdot f_1(x) + k^*_{p3}(x)\cdot f_2(x) + k^*_{i1}(x)\cdot\left[\int x_1\cdot dt\right]$$

$$+ \; k_{i2}^{*}(x)\cdot\left[\int f_1(x)\cdot dt\right] \tag{5.34}$$

$$k_{p1}^{*}(x) = \frac{k_{p1}}{\gamma\cdot f_{12}(x_1,x_2)} \tag{5.35}$$

$$k_{p2}^{*}(x) = \frac{k_{p2}}{\gamma\cdot f_{12}(x_1,x_2)} \tag{5.36}$$

$$k_{p3}^{*}(x) = -\frac{f_{11}(x_1,x_2)\cdot f_1(x_1,x_2)}{\gamma\cdot f_{12}(x_1,x_2)\cdot f_2(x_1,x_2)} - \frac{1}{\gamma} \tag{5.37}$$

$$k_{i1}^{*}(x) = \frac{k_{i1}}{\gamma\cdot f_{12}(x_1,x_2)} \tag{5.38}$$

$$k_{i2}^{*}(x) = \frac{k_{i2}}{\gamma\cdot f_{12}(x_1,x_2)} \tag{5.39}$$

and the approximations $f_1(x) = \dot{x}_1$, $f_2(x) = \dot{x}_2$, and constant gains are made, then the resulting controller is given by:

$$u = k_1\cdot x_1 + k_2\cdot\left[\int x_1\cdot dt\right] + k_3\cdot\dot{x}_1 + k_4\cdot\dot{x}_2 \tag{5.40}$$

This shows that the nonlinear PI controller resembles a two input PID controller with variable gains. The gains are scheduled as functions of x_1 and x_2, which were previously defined as deviations from the chosen equilibrium values of the reactor concentration c and the reactor temperature T, respectively. This nonlinear PI controller doesn't have the same form as the nonlinear PID controller. It assumes a known state and the variable integrator gain is not generated in the same way.

As can be determined from the various design schemes presented in this chapter and

the one presented in this thesis, all of these design schemes use controllers where some or all of the gains can be varied. The details of the design scheme can vary widely, depending on the aspects of the problem to be solved and the determination of the control law. However, in all cases the design schemes result in gain scheduling that involves the output or states of the plant. The nonlinear PID presented in this thesis uses gain scheduling based on the input to the plant. In addition the controllers presented in this chapter are concerned with a single equilibrium point whereas the nonlinear PID controller is designed to operate over a wide range of equilibrium points. This leads to the conclusion that, although gain scheduled controllers have been studied previously in the literature, the nonlinear PID controller presented here does not provide a unified framework. Also, since the controllers presented in this chapter are designed to operate at a single equilibrium point, these other nonlinear controller schemes are not capable of solving the control problem associated with the system described in Chapter 4.

CHAPTER 6

Conclusions

The results of the simulations of the ideal CSTR in Chapter 4 help support the argument that a simple controller works as well as a complex controller. The nonlinear PID controller will operate a system that fails under the control of a single linear controller. It also performs as well as a nonlinear IMC controller, which is much more complex than the nonlinear PID controller.

The simulations of the constant volume, non-adiabatic CSTR in Chapter 3 produced some unexpected results. A single linear PID controller performed better than a state feedback controller on a nonlinear system at certain initial conditions. This leads to the conclusion that the performance of a linear output feedback based controller can be better than the performance of a state feedback based controller for certain nonlinear systems.

The other nonlinear PID controllers detailed in Chapter 5 revealed a variety of schemes for improving performance of the classical PID algorithm. However, the nonlinear PID controller presented here did not provide a common framework with these other control schemes. One reason was that the nonlinear PID controller in this thesis scheduled gains as a function of the plant input, while the other controller schemes scheduled gains as a function of the plant output. Another reason was the fact that the other controller schemes were designed to operate near one particular equilibrium point, not a range of equilibrium points like the nonlinear PID controller presented here.

Future investigation could lead to improving the controller performance. One

suggestion is modifying the gain variations near system sign changes such that the system remains controlled and responds faster to removal of the parameter disturbance. Another suggestion is the use of cubic splines to approximate the nonlinear gain functions. This would result in a smoother approximation and might reduce any problems with sudden gain changes in the neighborhood of a selected design point.

BIBLIOGRAPHY

Alvarez, Jesús, Jaime Alvarez and Estela González. "Global Nonlinear Control of a Continuous Stirred Tank Reactor." Chemical Engineering Science 44, no. 5 (1989): 1147-1160.

Baumann, William T. "Discrete-Time Control of Continuous- Time Nonlinear Systems." Department of Electrical Engineering, Virginia Polytechnic Institute and State University August 14, 1989.

Biernson, George. Advanced Control Topics. Vol. 2 of Principles of Feedback Control. New York: John Wiley & Sons, 1988.

Clark, D. W. "PID Algorithms and their Computer Implementation." Transactions of the Institute of Measurement and Control 6, no. 6 (October-December 1984): 305-316.

Doyle, Francis J.,III, Andrew K. Packard and Manfred Morari. "Robust Controller Design for a Nonlinear CSTR." Chemical Engineering Science 44, no. 9 (1989): 1929-1947.

Economou, Constantin G., Manfred Morari and Bernhard O. Palsson. "Internal Model Control. 5. Extension to Nonlinear Systems." Industrial Engineering Chemical

Process Design and Development 25, no. 2 (1986): 403-411.

Gunzburger, Max. "Introduction to Numerical Analysis." Class Notes, MATH 4446. V.P.I.S.U., Spring 1990.

Hoo, K. A., and J. C. Kantor. Chemical Engineering Communications 37 (1985): 1

Hughes, F. M. "Self-tuning and Adaptive Control-a Review of Some Basic Techniques." Transactions of the Institute of Measurement and Control 8, no. 2 (April-June 1986): 100-110.

Jutan, Arthur. "A Nonlinear PI(D) Controller." The Canadian Journal of Chemical Engineering 67 (June 1989): 485-493.

Marini, Luigi and Christos Georgakis. "Low-Density Polyethylene Vessel Reactors." American Institute of Chemical Engineers Journal 30, no. 3 (May 1984): 401-415.

Rugh, W. J. "Design of Nonlinear PID Controllers." American Institute of Chemical Engineers Journal 33, no. 10 (October 1987): 1738-1742.

Wiberg, Donald M. Schaum's Outline of Theory and Problems of State Space and Linear Systems. McGraw-Hill, 1971.

VITA

I was born on June 20, 1962 in Columbia, SC but have lived most of my life in Newport News, VA. I attended Thomas Nelson Community College in Hampton, VA from September 1983 to June 1985 and graduated Magna Cum Laude with a A.A.S. in Electrical Technology. I held a summer job at Army Communicative Systems, Fort Eustis, VA from June to August 1985. I attended Old Dominion University as an undergraduate from August 1985 to December 1987 and graduated with a B.S. in Electrical Engineering Technology. During the summer of 1986 I held a summer job overseas at Kalmar Verkstad AB, Kalmar, Sweden. After some post-graduate work at Old Dominion from January to May 1988 I was accepted at V.P.I.S.U. in August 1988 as a graduate student in electrical engineering.

Nicholas D. Murray, Jr.